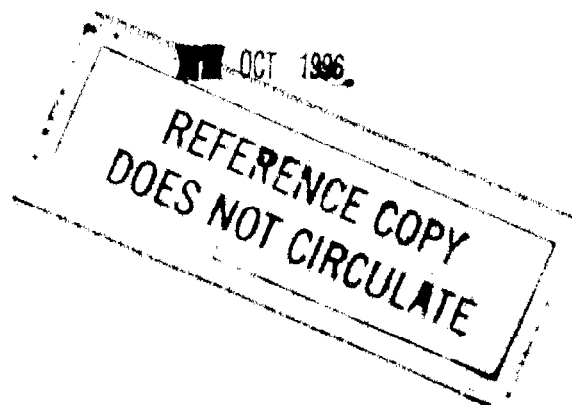# BRL

AD

CONTRACT REPORT NO. 343

EPIC-3, A COMPUTER PROGRAM FOR ELASTIC-
PLASTIC IMPACT CALCULATIONS IN 3
DIMENSIONS

Prepared by

Honeywell Inc., Defense Systems Division
600 Second Street Northeast
Hopkins, MN 55343

July 1977

Approved for public release; distribution unlimited.

USA ARMAMENT RESEARCH AND DEVELOPMENT COMMAND
USA BALLISTIC RESEARCH LABORATORY
ABERDEEN PROVING GROUND, MARYLAND

SECURITY CLASSIFICATION OF THIS PAGE (WHEN DATA ENTERED)

REPORT DOCUMENTATION PAGE		READ INSTRUCTIONS BEFORE COMPLETING FORM
1. REPORT NUMBER BRL CONTRACTOR REPORT NO. 343	2. GOV'T ACCESSION NUMBER	3. RECIPIENT'S CATALOG NUMBER
4. TITLE (AND SUBTITLE) EPIC-3, A COMPUTER PROGRAM FOR ELASTIC-PLASTIC IMPACT CALCULATIONS IN 3 DIMENSIONS.		5. TYPE OF REPORT/PERIOD COVERED Final - Jan. 1976-Feb. 1977
		6. PERFORMING ORG. REPORT NUMBER 47052
7. AUTHOR(S) Gordon R. Johnson		8. CONTRACT OR GRANT NUMBER(S) DAAD05-76-C-0747
9. PERFORMING ORGANIZATIONS NAME/ADDRESS Honeywell Inc., Defense Systems Division 600 Second Street Northeast Hopkins, Minnesota 55343		10. PROGRAM ELEMENT,PROJECT,TASK AREA & WORK UNIT NUMBERS
11. CONTROLLING OFFICE NAME/ADDRESS USA Ballistic Research Laboratory Aberdeen Proving Ground, MD 21005		12. REPORT DATE JULY 1977
		13. NUMBER OF PAGES 86
14. MONITORING AGENCY NAME/ADDRESS (IF DIFFERENT FROM CONT. OFF.) USA Materiel Development & Readiness Command 5001 Eisenhower Avenue Alexandria, VA 22333		15. SECURITY CLASSIFICATION (OF THIS REPORT) UNCLASSIFIED
		15a. DECLASSIFICATION DOWNGRADING SCHEDULE

16. DISTRIBUTION STATEMENT (OF THIS REPORT)

Approved for public release: distribution unlimited

17. DISTRIBUTION STATEMENT (OF THE ABSTRACT ENTERED IN BLOCK 20, IF DIFFERENT FROM REPORT)

18. SUPPLEMENTARY NOTES

19. KEY WORDS (CONTINUE ON REVERSE SIDE IF NECESSARY AND IDENTIFY BY BLOCK NUMBER)

Impact
Penetration
Wave Propagation
Finite Element

Lagrangian
Elastic-Plastic
Hydrodynamic

20. ABSTRACT (CONTINUE ON REVERSE SIDE IF NECESSARY AND IDENTIFY BY BLOCK NUMBER)

A three-dimensional computer program for high-velocity impact problems is described. The numerical technique is based on a Lagrangian finite-element formulation in which the equations of motion are integrated directly rather than through the traditional stiffness matrix approach. Tetrahedron elements are formulated for large strains and displacements, and nonlinear material strength and compressibility effects are included to account for elastic-plastic flow and wave propagation. A sliding surfaces capability is also included.

HD-168 REV 11/74

DD FORM 1 JAN 73 **1473** EDITION OF 1 NOV 55 IS OBSOLETE

SECURITY CLASSIFICATION OF THIS PAGE (WHEN DATA ENTERED)

FOREWORD

This final report on the formulation of EPIC-3, a
three-dimensional computer code for dynamic analyses
of high-velocity impact problems, was prepared by
Honeywell Inc., Defense Systems Division, for the
U.S. Army Ballistics Research Laboratories, Terminal
Ballistics Laboratory, under contract DAAD05-76-C-0747.
The period covered by the report is January 1976 to
February 1977.

The author, Gordon R. Johnson, would like to thank
J. A. Zukas of BRL and J. H. Blackburn of Honeywell
for their many helpful comments, suggestions and
discussions in developing EPIC-3 and this report.

CONTENTS

ILLUSTRATIONS

SECTION I
INTRODUCTION AND SUMMARY

This report documents a three-dimensional computer code which can be used for dynamic analyses of high-velocity impact problems. The code, EPIC-3 (Elastic-Plastic Impact Calculations in 3 dimensions), is based on a Lagrangian finite-element formulation where the equations of motion are integrated directly rather than through the traditional stiffness matrix approach. Nonlinear material strength and compressibility effects are included to account for elastic-plastic flow and wave propagation. Although this code is arranged to provide solutions for projectile-target impact problems, the basic formulation is valid for a wide range of problems involving dynamic responses of continuous media.

The EPIC-3 code has material descriptions which include strain hardening, strain rate effects, thermal softening and fracture. Geometry generators are included to generate quickly flat plates and rods with blunt, rounded or conical nose shapes. It has the capacity to include multiple sliding surfaces, it is restartable, and it provides cross-sectional plots of the deformed geometry.

A desirable characteristic of this technique is that there is no need to provide an orderly arrangement of nodes as is required for finite-difference techniques. Complex geometrical shapes can be represented simply by providing an adequate assemblage of elements to represent the geometry. Various boundary conditions can also be represented in a straightforward manner. Another desirable characteristic is that this technique is formulated for a tetrahedron element, which is well suited to represent the severe distortions which often occur during high-velocity impact. A tetrahedron element also provides a state of constant strain such that all

1

material in an element behaves uniformly. This allows for an accurate and convenient selection of a constant stress within the element.

This report includes a complete description and formulation of the EPIC-3 computer code. Detailed instructions for using this code are also provided.

SECTION II

FORMULATION

The EPIC-3 computational technique is shown schematically in Figure 1.
The first step in the process is to represent the geometry with tetrahedron
elements having specific material characteristics. Then the distributed
mass is lumped at the nodes (element corners), and initial velocities are
assigned to represent the motion at impact.

INITIAL CONDITIONS   INTEGRATION LOOP

Figure 1. Basic Computational Technique
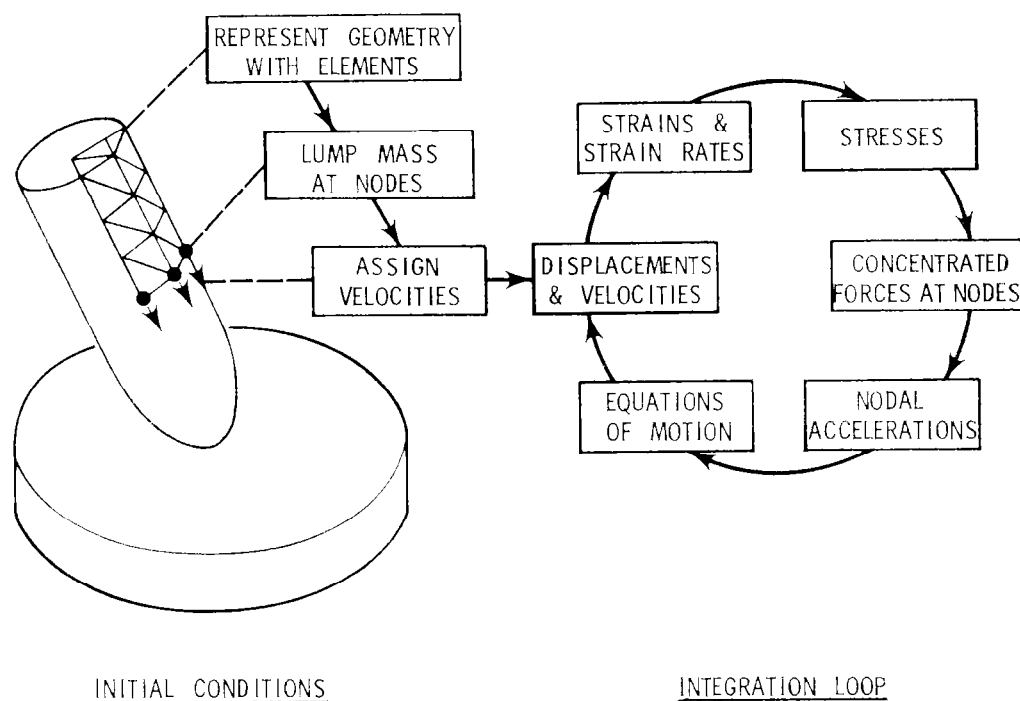
After the initial conditions are established, the integration loop begins as
shown in Figure 1. The first step is to obtain displacements and velocities
of the nodes. If it is assumed the lines connecting the nodes (element edges)
remain straight, then the displacements and velocities within the elements
must vary linearly. From these displacements and velocities, the strains

3

and strain rates within the elements can be obtained. Since the strains and strain rates are derivatives of linear displacement and velocity functions within the elements, the resulting strains and strain rates are constant within the elements.

The stresses in the elements are determined from the strains, strain rates, internal energies and material properties. Since the strains and strain rates are constant within the elements, the stresses are also constant. If the strains are in the elastic range, the elastic stresses can be obtained in a straightforward manner from Hooke's law. For larger strains, involving plastic flow, the stresses are obtained by combining plastic deviator stresses with hydrostatic pressure. The plastic deviator stresses represent the shear-strength capability of the material, and the hydrostatic pressure is obtained from the volumetric strain and internal energy of the element. An artificial viscosity is also included to damp out localized oscillations caused by representing continuous media with lumped masses.

After the element stresses are determined, it is necessary to obtain concentrated forces at the nodes. These forces are statically equivalent to the distributed stresses within the element and are dependent on the element geometry and the magnitude of the stresses. When the concentrated forces are applied to the concentrated masses, the nodal accelerations are defined, and the equations of motion are applied to determine new displacements and velocities. The integration loop is then repeated until the time of interest has elapsed.

An important additional feature of the basic technique is the ability to represent sliding between two surfaces. This is accomplished with a momentum exchange principle which allows for closing and separation of the two surfaces. It should be noted that the integration time increment must be properly controlled to prevent numerical instability. This is accomplished by limiting the time increment to a fraction of the time required to travel across the minimum altitude of the element at the sound velocity of the material. This also ensures that the time increment is less than the lowest period of vibration of the system.

4

2.1 GEOMETRY

A typical tetrahedron element is shown in Figure 2. It is geometrically defined by nodes i, j, m, and p. The formulation is based on nodes i, j, and m being positioned in a counterclockwise manner when viewed from node p. For the initial geometry, the coordinates of node i are defined by x_i^o, y_i^o, and z_i^o. The coordinates of node i for the displaced geometry are given by x_i, y_i, and z_i. In all cases, the superscript "o" is used to designate the initial condition. The displacement of node i along the x axis is $u_i = x_i -x_i^o$, and the y and z displacements are given by $v_i = y_i - y_i^o$ and $w_i = z_i - z_i^o$. The lumped mass at each of the four nodes is

$$M_i' = M_j' = M_m' = M_p' = \frac{1}{4} V^o \rho^o \tag{1}$$

where V^o and ρ^o are the initial volume and density of the element. The individual elements can be assembled by use of geometry generators described in subsection 4.1. When all elements are completely assembled to form a continuous medium, the total mass at node i is $M_i = \sum M_i'$.

2.2 STRAINS AND STRAIN RATES

The strains are obtained from the initial geometry of the element and the displacements of the nodes. If it is assumed the displacements vary linearly between the nodes, the x, y and z displacements (u, v, w) can be expressed as

$$u = \alpha_1 + \alpha_2 x + \alpha_3 y + \alpha_4 z \tag{2}$$

$$v = \alpha_5 + \alpha_6 x + \alpha_7 y + \alpha_8 z \tag{3}$$

$$w = \alpha_9 + \alpha_{10} x + \alpha_{11} y + \alpha_{12} z \tag{4}$$
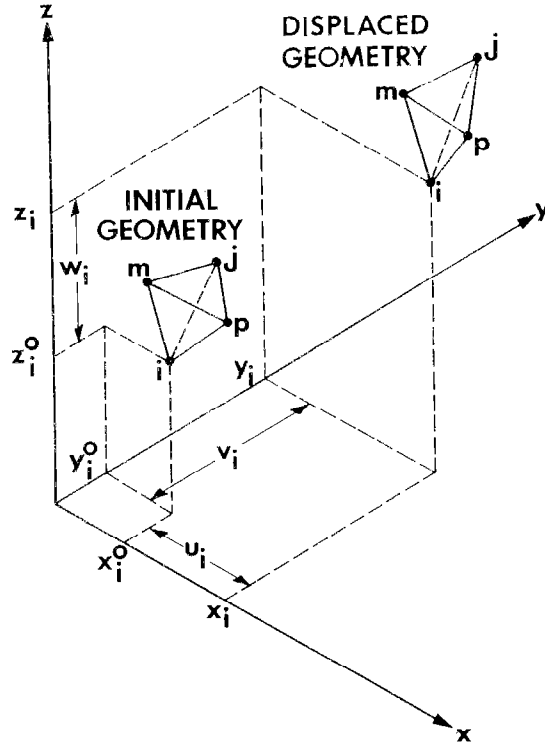
Figure 2. Geometric Properties of a Tetrahedron Element

where $\alpha_1 \ldots \alpha_{12}$ are geometry- and displacement-dependent constants. It is possible to solve for $\alpha_1 \ldots \alpha_4$ by substituting the x displacements and initial coordinates of the four nodes into Equation (2). This gives four equations and four unknowns so that the constants $(\alpha_1 \ldots \alpha_4)$ can be evaluated.

Equation (2) can then be expressed in terms of element geometry and nodal displacements.

$$
\begin{aligned}
u = \frac{1}{6V^o} \Bigg[&(a_i^o + b_i^o x + c_i^o y + d_i^o z)\, u_i \\
+ \quad &(a_j^o + b_j^o x + c_j^o y + d_j^o z)\, u_j \\
+ \quad &(a_m^o + b_m^o x + c_m^o y + d_m^o z)\, u_m \\
+ \quad &(a_p^o + b_p^o x + c_p^o y + d_p^o z)\, u_p \Bigg]
\end{aligned}
\tag{5}
$$

6

where the initial volume is

$$V^O = \frac{1}{6} \begin{vmatrix} 1 & x_i^O & y_i^O & z_i^O \\ 1 & x_j^O & y_j^O & z_j^O \\ 1 & x_m^O & y_m^O & z_m^O \\ 1 & x_p^O & y_p^O & z_p^O \end{vmatrix} \qquad (6a)$$

and the other geometry-dependent constants are

$$a_i^O = \begin{vmatrix} x_j^O & y_j^O & z_j^O \\ x_m^O & y_m^O & z_m^O \\ x_p^O & y_p^O & z_p^O \end{vmatrix} \qquad (6b)$$

$$b_i^O = - \begin{vmatrix} 1 & y_j^O & z_j^O \\ 1 & y_m^O & z_m^O \\ 1 & y_p^O & z_p^O \end{vmatrix} \qquad (6c)$$

$$c_i^O = \begin{vmatrix} 1 & x_j^O & z_j^O \\ 1 & x_m^O & z_m^O \\ 1 & x_p^O & z_p^O \end{vmatrix} \qquad (6d)$$

7

$$d_i^o = - \begin{vmatrix} 1 & x_j^o & y_j^o \\ 1 & x_m^o & y_m^o \\ 1 & x_p^o & y_p^o \end{vmatrix} \qquad (6e)$$

The remaining geometry-dependent constants (a_j^o, b_j^o, c_j^o, d_j^o, etc.) are obtained by a systematic interchange of signs and subscripts. The y and z displacements in Equations (3) and (4) are obtained in a similar manner and are identical to Equation (5) except the x displacements are replaced by the y and z displacements.

After the displacements are obtained, it is possible to determine the strains within the elements from the following equations (Ref. 1):

$$\epsilon_x = \frac{\partial u}{\partial x} + \frac{1}{2} \left[\left(\frac{\partial u}{\partial x} \right)^2 + \left(\frac{\partial v}{\partial x} \right)^2 + \left(\frac{\partial w}{\partial x} \right)^2 \right] \qquad (7)$$

$$\epsilon_y = \frac{\partial v}{\partial y} + \frac{1}{2} \left[\left(\frac{\partial u}{\partial y} \right)^2 + \left(\frac{\partial v}{\partial y} \right)^2 + \left(\frac{\partial w}{\partial y} \right)^2 \right] \qquad (8)$$

$$\epsilon_z = \frac{\partial w}{\partial z} + \frac{1}{2} \left[\left(\frac{\partial u}{\partial z} \right)^2 + \left(\frac{\partial v}{\partial z} \right)^2 + \left(\frac{\partial w}{\partial z} \right)^2 \right] \qquad (9)$$

$$\gamma_{xy} = \frac{\partial u}{\partial y} + \frac{\partial v}{\partial x} + \frac{\partial u}{\partial x}\frac{\partial u}{\partial y} + \frac{\partial v}{\partial x}\frac{\partial v}{\partial y} + \frac{\partial w}{\partial x}\frac{\partial w}{\partial y} \qquad (10)$$

$$\gamma_{xz} = \frac{\partial u}{\partial z} + \frac{\partial w}{\partial x} + \frac{\partial u}{\partial x}\frac{\partial u}{\partial z} + \frac{\partial v}{\partial x}\frac{\partial v}{\partial z} + \frac{\partial w}{\partial x}\frac{\partial w}{\partial z} \qquad (11)$$

$$\gamma_{yz} = \frac{\partial v}{\partial z} + \frac{\partial w}{\partial y} + \frac{\partial u}{\partial y}\frac{\partial u}{\partial z} + \frac{\partial v}{\partial y}\frac{\partial v}{\partial z} + \frac{\partial w}{\partial y}\frac{\partial w}{\partial z} \qquad (12)$$

$$\epsilon_v = \frac{V}{V^o} - 1 \qquad (13)$$

The normal strains are represented by Equations (7) through (9), the shear strains by Equations (10) through (12), and the volumetric strain by Equation (13). The higher-order terms are required to represent the effect of element rotation.

The strains in Equations (7) through (12) are determined as functions of the displacements by taking partial derivatives of Equations (2) through (4), and substituting them into the strain equations. These strains consist of derivatives of linear equations and are therefore constant (functions of α_1 . . . α_{12} only) within the element. It is also necessary to use an equivalent strain which is expressed as

$$\bar{\epsilon} = \sqrt{\frac{2}{9} \left[(\epsilon_x - \epsilon_y)^2 + (\epsilon_x - \epsilon_z)^2 + (\epsilon_y - \epsilon_z)^2 + \frac{3}{2} (\gamma_{xy}^2 + \gamma_{xz}^2 + \gamma_{yz}^2) \right]} \qquad (14)$$

This strain provides an overall measure of the distortion of the element and can be used to obtain strain hardening stresses which occur during plastic flow (Ref. 2).

The strain rates are obtained in a manner similar to that used to determine the strains. Since the velocities ($\dot{u}$, $\dot{v}$, $\dot{w}$) also vary linearly between the nodes, the basic form of Equations (2) through (12) is used, except the nodal velocities are substituted for the nodal displacements and the higher-order terms are dropped. Also, the displaced geometry is used so that the geometry-dependent constants in Equation (6) are obtained from the displaced coordinates (x_i, y_i, z_i, etc.) rather than the initial coordinates (x_i^o, y_i^o, z_i^o, etc.). The resulting constants for the displaced geometry are designated as a_i, b_i, c_i, d_i, etc. The normal strain rates ($\dot{\epsilon}_x$, $\dot{\epsilon}_y$, $\dot{\epsilon}_z$) are adjusted into deviator strain rates ($\dot{e}_x$, $\dot{e}_y$, $\dot{e}_z$), and the shear strain rates are represented by $\dot{\gamma}_{xy}$, $\dot{\gamma}_{xz}$, and $\dot{\gamma}_{yz}$.

2.3 STRESSES

The stresses in the elements are determined from the strains, strain rates, internal energies, and material properties. The <u>elastic stresses</u> can be obtained directly from the strains by use of Hooke's Law (Ref. 2):

$$\sigma_x = \lambda \epsilon_v + 2G\epsilon_x - Q \tag{15}$$

$$\sigma_y = \lambda \epsilon_v + 2G\epsilon_y - Q \tag{16}$$

$$\sigma_z = \lambda \epsilon_v + 2G\epsilon_z - Q \tag{17}$$

$$\tau_{xy} = G\gamma_{xy} \tag{18}$$

$$\tau_{xz} = G\gamma_{xz} \tag{19}$$

$$\tau_{yz} = G\gamma_{yz} \tag{20}$$

where σ_x, σ_y and σ_z are the normal stresses, and τ_{xy}, τ_{xz} and τ_{yz} the shear stresses. Lame's elastic constants are λ and G, and the artificial viscosity, Q, will be defined later. The stresses are combined to form an equivalent stress given by

$$\bar{\sigma} = \sqrt{\frac{1}{2}\left[(\sigma_x - \sigma_y)^2 + (\sigma_x - \sigma_z)^2 + (\sigma_y - \sigma_z)^2 + 6(\tau_{xy}^2 + \tau_{xz}^2 + \tau_{yz}^2)\right]} \tag{21}$$

This stress is analogous to the equivalent strain of Equation (14) inasmuch as it represents an overall state of stress within the element (Ref. 2). If $\bar{\sigma}$ is less than the tensile yield strength of the material, the stresses are in the elastic range. It should be noted that the elastic stresses are dependent on strains which are relative to the rotated orientation of the element. Generally, the element rotation is very small while it is in the elastic range and no compensation is required. If significant rotations are experienced in the elastic range, however, a transformation of the stresses would be necessary.

Plastic flow begins when the elastic strength of the material is exceeded. In conjunction with the plastic flow, allowance is also made to include the effect of viscosity. For these cases the normal stresses are obtained by combining the plastic and viscous deviator stresses with the hydrostatic pressure and artificial viscosity. This gives

$$\sigma_x = s_x - (P + Q) \tag{22}$$

$$\sigma_y = s_y - (P + Q) \tag{23}$$

$$\sigma_z = s_z - (P + Q) \tag{24}$$

where s_x, s_y and s_z are the deviator stresses, P is the hydrostatic pressure and Q is the artificial viscosity.

The deviator stresses represent the shear strength characteristics of the material. By using the von Mises incremental theory of plasticity (Ref. 2) and the Navier-Strokes equations (Ref. 3), the deviator stresses (s_x, s_y, s_z) and shear stresses (τ_{xy}, τ_{xz}, τ_{yz}) are given by

$$s_x = \frac{2}{3}\left(\frac{\dot{e}_x}{\dot{\bar{\epsilon}}}\right)\bar{S} + 2\bar{V}\dot{e}_x \tag{25}$$

$$s_y = \frac{2}{3}\left(\frac{\dot{e}_y}{\dot{\bar{\epsilon}}}\right)\bar{S} + 2\bar{V}\dot{e}_y \tag{26}$$

$$s_z = \frac{2}{3}\left(\frac{\dot{e}_z}{\dot{\bar{\epsilon}}}\right)\bar{S} + 2\bar{V}\dot{e}_z \tag{27}$$

$$\tau_{xy} = \frac{1}{3}\left(\frac{\dot{\gamma}_{xy}}{\dot{\bar{\epsilon}}}\right)\bar{S} + \bar{V}\dot{\gamma}_{xy} \tag{28}$$

$$\tau_{xz} = \frac{1}{3}\left(\frac{\dot{\gamma}_{xz}}{\dot{\bar{\epsilon}}}\right)\bar{S} + \bar{V}\dot{\gamma}_{xz} \tag{29}$$

$$\tau_{yz} = \frac{1}{3}\left(\frac{\dot{\gamma}_{yz}}{\dot{\bar{\epsilon}}}\right)\bar{S} + \bar{V}\dot{\gamma}_{yz} \tag{30}$$

The first terms in Equations (25) through (30) represent the plastic strength where $\overline{S}$ is the equivalent tensile strength of the material and $\overline{\epsilon}$ is the equivalent strain rate, which is analogous to the equivalent strain in Equation (14). The second terms represent the viscous effects where $\overline{V}$ is the absolute viscosity of the material. For the case of no viscosity ($\overline{V} = 0$), if the stresses in Equations (22) through (24) and Equations (28) through (30) are substituted into Equation (21), the result is always $\overline{\sigma} = \overline{S}$. It should be noted that the sum of the deviator strain rates is equal to zero, and, since the deviator stresses are directly proportional to the deviator strain rates, the sum of the deviator stresses is also equal to zero. The net pressure in the element is therefore not affected by the deviator stresses.

The equivalent tensile strength of the material may be dependent on many factors, including strain, strain rate, pressure and temperature. It is well-known that many materials behave differently under dynamic impact than under static testing conditions. With few exceptions, however, a precise definition of material behavior under dynamic conditions is not available. There is also much to be learned about fracture characteristics under these dynamic conditions. This version of EPIC-3 allows the equivalent tensile strength to be determined from

$$\overline{S} = S_{\overline{\epsilon}} \left[1 + C_1 \log (\tilde{\epsilon}) \right] \left[1 + C_2 \mu + C_3 \mu^2 \right] \left[C_4 + C_5 T \right] \tag{31}$$

In this formulation, $S_{\overline{\epsilon}}$ is generally taken to be the static stress, which is dependent on the equivalent strain of Equation (14). It is generally necessary to calculate $\tilde{\epsilon}$ on a path-dependent basis, rather than the path-independent basis of Equation (14). For most impact problems, however, when distortions are severe there is little recovery of strains and this is an adequate approximation.

The three bracketed terms allow the static stress to be altered, based on strain rate, pressure and temperature. If the constants are $C_1 = C_2 = C_3 = C_5 = 0$ and $C_4 = 1.0$, then $\overline{S} = S_{\overline{\epsilon}}$, which is the strain dependent static stress. The first bracketed term can increase the strength due to the equivalent strain rate, $\dot{\overline{\epsilon}}$, described earlier. In the second bracketed term, $\mu = \rho/\rho^0 - 1 = V^0/V - 1$. Since the hydrostatic pressure will be shown to be primarily dependent on μ, the effect of this term is to increase the strength due to pressure. The final bracketed term includes the temperature, T, of the element, which is obtained from the nonrecoverable work done in the element by the artificial viscosity and the plastic and viscous deviator stresses. This term tends to reduce the strength. The formulations for the nonrecoverable work and temperature are presented later in subsection 2.7.

Material fracture is currently dependent on the equivalent strain, $\overline{\epsilon}$, and the volumetric strain, ϵ_V. When the fracture criterion has been met, the equivalent tensile stress is set equal to zero, so that no shear stresses can be developed in the failed element. Likewise, no tensile stresses are allowed to develop. The net result is that a failed element tends to act like a liquid inasmuch as it can develop only hydrostatic compression with no shear or tensile stresses. Another option is also available which sets all stresses (including the pressure) equal to zero.

It is recognized that other more sophisticated material descriptions are being developed. It should be noted that the EPIC-3 formulation is ideally suited to incorporate additional material models. The entire tetrahedron element is in a uniform state of constant strain and has associated with it the parameters such as strains, strain rates, internal energy and temperature. From these parameters, the stresses in the element can readily be obtained by various selected formulations.

The hydrostatic pressure is dependent on the volumetric strain and the internal energy in the element. The EPIC-3 code uses the Mie-Grüneisen equation of state in the following form (Ref. 4):

$$P = \left(K_1\mu + K_2\mu^2 + K_3\mu^3\right)\left(1 - \frac{\Gamma\mu}{2}\right) + \Gamma E_s\left(1 + \mu\right) \tag{32}$$

The internal energy per original unit volume, E_s, is obtained from the element by the various stresses and is formulated later in 2.7; K_1, K_2, and K_3 are material-dependent constants, and Γ is the Grüneisen coefficient.

The artificial viscosity is combined with the normal stresses to damp out localized oscillations of the concentrated masses. It tends to eliminate spurious oscillations which would otherwise occur for wave propagation problems. This technique was originally proposed by Von Neumann and Richtmyer (Ref. 5) and has been expanded for use in various computer codes (Ref. 6, 7). It is expressed in terms of linear and quadratic components and is applied only when the volumetric strain rate is negative:

$$Q = C_L \rho c_s h \left|\dot{\epsilon}_v\right| + C_o^2 \rho h^2 (\dot{\epsilon}_v)^2 \qquad \text{for } \dot{\epsilon}_v < 0 \tag{33}$$

$$Q = 0 \quad \text{for } \dot{\epsilon}_v \geq 0$$

where c_s is the sound velocity of the material and h is the minimum altitude of the tetrahedron. Typical values used for the dimensionless coefficients are $C_L = 0.5$ and $C_o^2 = 4.0$.

The minimum altitude of the tetrahedron can readily be obtained from the previously calculated geometry-dependent constants. The altitude from node i to the plane defined by the other three nodes of the tetrahedron is

$$h_i = \frac{6V}{\sqrt{b_i^2 + c_i^2 + d_i^2}} \tag{34}$$

The other altitudes (h_j, h_m, h_p) are obtained by appropriately changing the subscripts of the geometry dependent constants.

14

The sound velocity is dependent on the state of the material (elastic or plastic) and is defined as follows:

$$c_s = \sqrt{(\lambda + 2G)/\rho^0} \tag{35a}$$

$$c_s = \sqrt{(K_1 + 2K_2\mu + 3K_3\mu^2)/\rho^0} \tag{35b}$$

2.4 CONCENTRATED FORCES

After the element stresses are determined, the concentrated nodal forces can be obtained. These forces are statically equivalent to the distributed stresses within the element and are dependent on the displaced element geometry and the magnitude of the stresses. The forces in the x, y and z directions at node i of an element, are given by

$$F_i^x = - \frac{1}{6} (b_i\sigma_x + c_i\tau_{xy} + d_i\tau_{xz}) \tag{36}$$

$$F_i^y = - \frac{1}{6} (c_i\sigma_y + b_i\tau_{xy} + d_i\tau_{yz}) \tag{37}$$

$$F_i^z = - \frac{1}{6} (d_i\sigma_z + c_i\tau_{yz} + b_i\tau_{xz}) \tag{38}$$

The geometry-dependent constants (b_i, c_i, d_i) are again identical to those used for calculation of the strain rates and altitudes. The forces at the other nodes are readily obtained by changing subscripts. The net forces at node i (ΣF_i^x, ΣF_i^y, ΣF_i^z) are the sum of the node i forces from each element which includes that node.

15

2.5 EQUATIONS OF MOTION

The equations of motion can be numerically integrated by assuming a constant velocity for each time increment. The acceleration of node i in the x direction at time = t is

$$\ddot{u}_i^{\,t} = \frac{\sum F_i^x}{M_i} \tag{39}$$

The new constant velocity for the next time increment is

$$\dot{u}_i^{\,t+} = \dot{u}_i^{\,t-} + \ddot{u}_i^{\,t}\,\Delta t \tag{40}$$

where $\dot{u}_i^{\,t-}$ is the constant velocity for the previous time increment and Δt is the integration time increment. Finally, the new displacement at time = $t + \Delta t$ is

$$u_i^{\,t+\Delta t} = u_i^{\,t} + \dot{u}_i^{\,t+}\,\Delta t \tag{41}$$

The equations of motion for the y and z directions have a similar form.

It should be noted that both translational and rotational momenta are conserved with this formulation. The concentrated forces of Equations (36) through (38) are in static equilibrium so that the net forces and moments associated with each element are equal to zero. Therefore, the net forces and moments acting on the entire system are also equal to zero if there are no external restraints or applied forces. Since the impulses acting on the nodes are simply the forces times the time increment, the net impulses are equal to zero, and the net translational and rotational momenta of the system are not altered.

The integration time increment used for the equations of motion is given by

$$\Delta t = C_t \left[\frac{h}{\sqrt{g^2} + \sqrt{g^2 + c_s^2}} \right] \tag{42}$$

where $g^2 = C_o^2 Q / \rho$, h is the previously determined minimum altitude, and c_s is the sound velocity. The constant, C_t, must be less than unity to ensure that Δt is always less than the time required to travel across the shortest dimension of the tetrahedron at the sound velocity of the material. Use of a time increment significantly larger than that specified by Equation (42) will lead to numerical instability (Ref. 7). The EPIC-3 program restricts the time increment from increasing more than 10 percent per cycle.

2.6 SLIDING SURFACES

It is sometimes necessary to allow for sliding to occur between two surfaces. A summary of the important steps for the sliding-surface technique follows:

- Identify a "master" sliding surface defined by an orderly arrangement of master nodes.

- Identify "slave" nodes which may slide along the master surface.

- For each integration time increment, apply the equations of motion to both the master nodes and the slave nodes in the usual manner.

- For each slave node, find the triangular plane (defined by three master nodes) whose projection contains that slave node.

- Check to determine if there is interference between the slave node and the master surface (the triangular plane defined by three master nodes).

17

- If there is interference, place the slave node on the master surface in a direction normal to the appropriate master triangular plane.

- Calculate the momentum change (impulse) to the slave node caused by placing it on the master surface; then transfer this lost momentum to the three surrounding master nodes.

The first step in the process is to define the master surface. It is generally desirable to define this surface with an orderly arrangement of nodes since a systematic search is required on this surface. An example of this is shown in the upper portion of Figure 3 where a flat plate is represented by a finite-element model of nodes and elements. The z-axis points vertically upward and the x and y axes are in a horizontal plane. Although the basic principles involved in this technique are independent of the orientation of the axes, the search technique is simplified if the z coordinates of the master surface are limited to a single-valued function of x and y (i.e., any vertical line, parallel to the z axis must not pass through the master surface at more than one point). Also, for this discussion, the slave surface is above the master surface relative to the z axis. Due to the symmetry of the plate about a plane containing the x and z axes, only half the plate is considered as shown. The EPIC-3 code uses a master surface defined by M rows of nodes, with each row containing N nodes. Looking downward from the positive z axis, the second row of nodes from N + 1 to 2N, is to the left of the first row of nodes going from 1 to N. Likewise, the third row is to the left of the second row, etc. For the specific case shown in Figure 3, N = 23 and M = 4, for a total of 92 master nodes.

It is also necessary to identify slave nodes for the other sliding surface. Since these nodes do not require an orderly arrangement, it is usually convenient to designate the more geometrically complex surface as the slave surface. It is also desirable to restrict the slave node spacing from becoming significantly greater than the master node spacing, because this could introduce localized deformations in the master surface at the slave node locations. Likewise, the mass of the slave nodes should not be significantly greater than the mass of the master nodes, since this could result in unrealistically high velocities of the master nodes at impact.

NODE (M − 1)•N + 1

MASTER SURFACE

NODE 1

NODE M•N

NODE N

k = 63

SLAVE NODE PROJECTION

i = 40   j = 41

70   92

Y

47   69

24   46

1   23
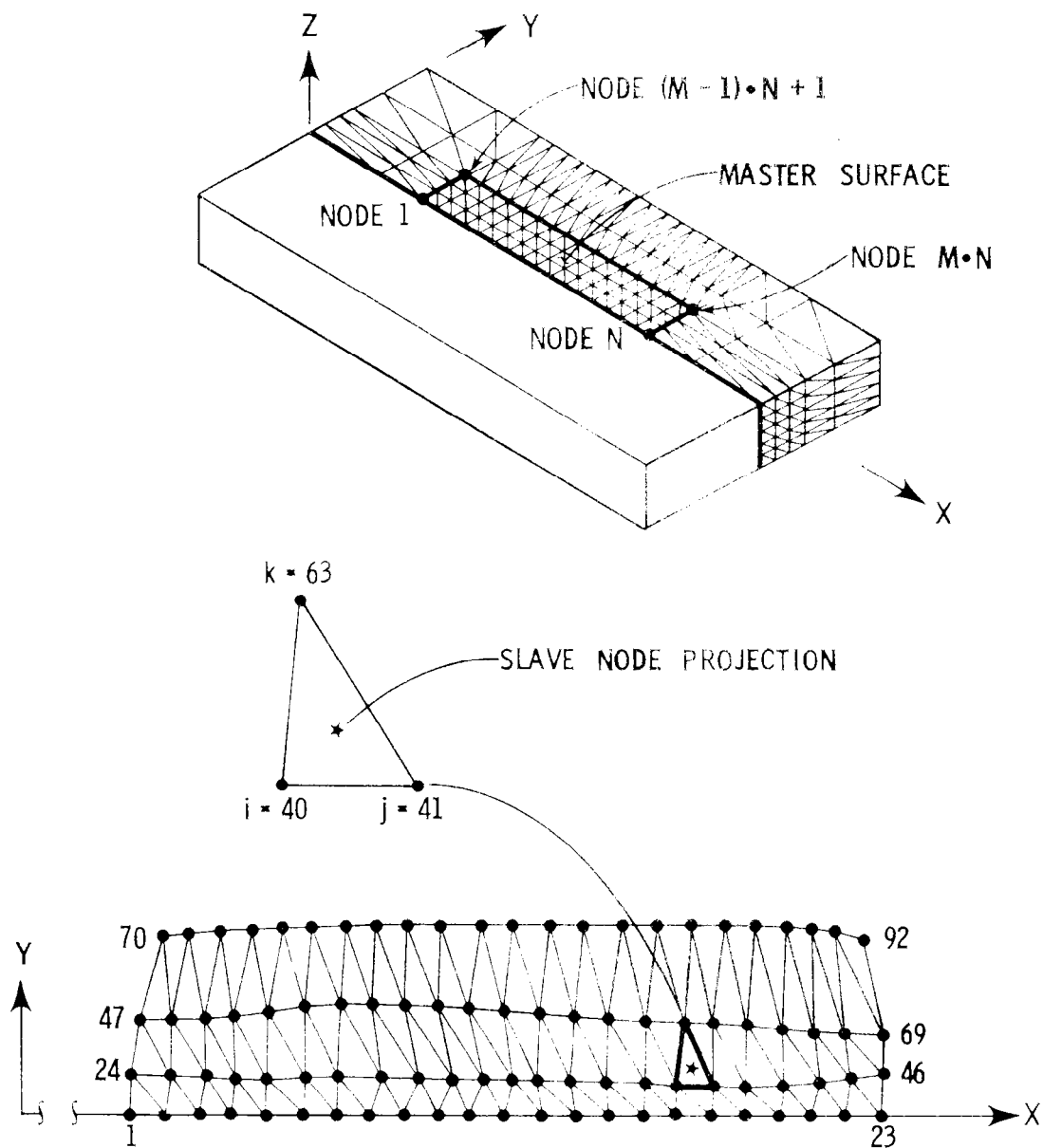
X-Y PROJECTION OF DISPLACED MASTER SURFACE

Figure 3.   Master Surface Geometric Representation

For each integration loop, the equations of motion are applied to both the master and slave nodes in the usual manner described in subsection 2.5. It is then necessary to check each slave node to determine if it has passed through the master surface, thus causing interference. To begin, the extreme values of the entire master surface are determined; if the slave node is not within this region, there can be no interference. If, for instance, the z coordinate of the slave node is greater than the maximum z coordinate of the master surface, there can be no interference, and the check for that particular slave node is complete.

If the slave node is within the confines of the master surface, a search through the master surface must be initiated. It is for this search that it is desirable to have an orderly arrangement of master nodes. The lower portion of Figure 3 shows the projection of an arbitrarily displaced master surface on the x-y plane. The triangular grid is consistent with the triangular faces of the tetrahedron elements. Since z is a single-valued function, there is no overlapping of triangles on the x-y projection. The objective of the search is to determine which triangle contains the x-y projection for each slave node. The search begins by considering the triangles between the first two rows of nodes. With reference to the lower portion of Figure 3, the first triangle is defined by nodes 1, 2, 24, the second by nodes 2, 25, 24, and the third by nodes 2, 3, 25, etc. If the slave node projection is not found by the last triangle in the row (nodes 23, 46, 45), the pattern is repeated in the second row of triangles beginning with the triangle defined by nodes 24, 25, 47.

An efficient way to check if the slave node projection is within a specific triangle is to determine the distance from the slave node to each of the lines defining the three sides of the triangle. The distance to line i-j, in the x-y plane, is given by

$$\delta_{xy} = \frac{\beta_1 x'_s + \beta_2 y'_s + \beta_3}{\sqrt{\beta_1^2 + \beta_2^2}} \tag{43}$$

where $\beta_1 = y_i - y_j$, $\beta_2 = x_j - x_i$ and $\beta_3 = x_i y_j - x_j y_i$. The coordinates of master node i are x_i, y_i and z_i, and the coordinates of the slave node are x_s', y_s', and z_s'. If master node j is counterclockwise from node i, when looking downward from the positive z axis, and δ_{xy} is positive for all three lines of the triangle, then the slave node is contained within the triangle. This is also illustrated in Figure 3 where the slave node is included in the triangle defined by nodes 40, 41 and 63.

After the appropriate triangle is identified, it is necessary to determine if there is interference. The equation of a plane through nodes i, j and k (taken counterclockwise, when looking downward from the positive z axis) is

$$Ax + By + Cz + D = 0 \qquad (44)$$

where

$$A = \begin{vmatrix} y_i & z_i & 1 \\ y_j & z_j & 1 \\ y_k & z_k & 1 \end{vmatrix} \qquad (45a)$$

$$B = - \begin{vmatrix} x_i & z_i & 1 \\ x_j & z_j & 1 \\ x_k & z_k & 1 \end{vmatrix} \qquad (45b)$$

$$C = \begin{vmatrix} x_i & y_i & 1 \\ x_j & y_j & 1 \\ x_k & y_k & 1 \end{vmatrix} \qquad (45c)$$

$$D = - \begin{vmatrix} x_i & y_i & z_i \\ x_j & y_j & z_j \\ x_k & y_k & z_k \end{vmatrix} \qquad (45d)$$

If the coordinates of the slave node are x_s', y_s', z_s', the corresponding z coordinate of the plane, z_p, can be obtained by rearranging Equation (44):

$$z_p = - \frac{D + Ax_s' + By_s'}{C} \qquad (46)$$

If z_p (master) is less than z_s' (slave), the surfaces are separated at this slave node location, and the final coordinates of the slave node (x_s, y_s, z_s) are simply equal to the initial coordinates (x_s', y_s', z_s') determined from the equations of motion. If, however, z_p is greater than z_s', there is interference, and the sliding process must be continued.

If there is interference, the next step is to place the slave node on the master surface in a direction normal to the master surface. This technique is illustrated in Figure 4 where a triangular plane is defined by master nodes i, j and k. The initial slave node position (x_s', y_s', z_s') lies below the triangular plane, as shown in the comparison between z_p and z_s'. A vector is shown which passes through the initial slave node position and is normal to the triangular plane. The three direction cosines of this vector are readily obtained by dividing A, B and C by $\sqrt{A^2 + B^2 + C^2}$. The slave node is moved a distance, δ_N, along this normal vector until it intersects the triangular plane. This normal distance is defined by

$$\delta_N = - \frac{Ax_s' + By_s' + Cz_s' + D}{\sqrt{A^2 + B^2 + C^2}} \qquad (47)$$

The final coordinates of the slave node are $x_s = x_s' + \Delta x$, $y_s = y_s' + \Delta y$ and $z_s = z_s' + \Delta z$, where Δx, Δy and Δz are obtained by multiplying δ_N by the appropriate direction cosines of the normal vector.

After geometric compatibility has been achieved by placing the slave node on the master surface, it is necessary to adjust the equations of motion to account for this change. Since the geometric changes are made only in the direction normal to the master plane, the equations of motion are altered only in this normal direction. No changes are made to the equations of

22
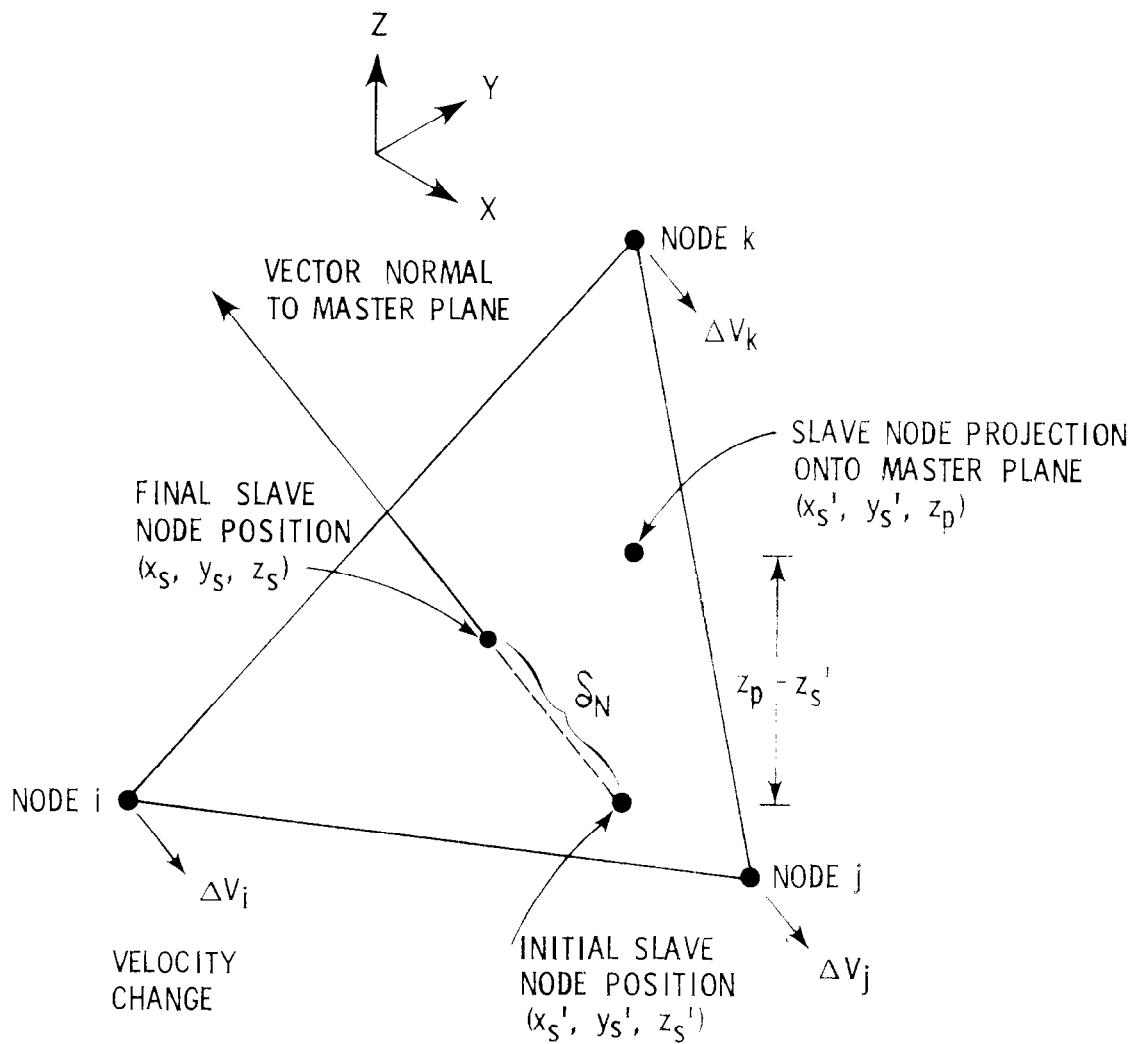
Figure 4. Slave Node Placement onto Master Surface

23

motion parallel to the master surface. This has the effect of assuming a frictionless surface.

In the process of moving the slave node to the master surface, an effective velocity change is imposed on the slave node. This loss of velocity in the normal direction is $\Delta V_N = \delta_N / \Delta t$, where Δt is the integration time increment for the previous cycle. This velocity change also gives a momentum change along the normal direction equal to $M_s \, \Delta V_N$, where M_s is the mass of the slave node. This momentum is then transferred to the three surrounding master nodes. If R_i, R_j and R_k represent the fractions of the momentum to be transferred to the three nodes, a summation of the translational and rotational momenta of the three nodes gives the following equations:

$$R_i + R_j + R_k = 1 \tag{48}$$

$$R_i \, (x_i - x_s) + R_j \, (x_j - x_s) + R_k \, (x_k - x_s) = 0 \tag{49}$$

$$R_i \, (y_i - y_s) + R_j \, (y_j - y_s) + R_k \, (y_k - y_s) = 0 \tag{50}$$

These three equations and three unknowns define the appropriate momentum distribution to the three nodes. This momentum is applied to the master nodes in the form of instantaneous velocity changes, parallel to the normal vector but in the opposite direction. For instance, the normal direction velocity change to node i is

$$\Delta V_i = R_i \, M_s \, \Delta V_N / M_i \tag{51}$$

where M_i is the mass of master node i, and M_s is the mass of the slave node. As was done for the displacements, the specific velocity changes in the x, y and z directions are obtained by multiplying ΔV_i by the appropriate direction cosines.

This is an extremely accurate technique because translational momenta are absolutely conserved in all three directions. Small errors are introduced

into the center of gravity (cg) positions when the slave node is moved to the master surface, since there is no corresponding movement of the master nodes, which receive only instantaneous velocity changes. This cg error also introduces small errors into the rotational momenta. The magnitude of these errors is identified in the example problem of subsection 2.9.

2.7 SYSTEM PARAMETERS

It is often desirable to examine system parameters such as cg positions, translational and rotational momenta, kinetic energy, plastic work and total energy. The EPIC-3 code calculates these parameters for the projectile, target and total system (projectile and target). The cg position in the x direction is given by

$$\bar{x} = \frac{\sum M_i x_i}{\sum M_i} \qquad (52)$$

where M_i and x_i are the mass and x coordinate of node i. The summation includes all nodes of the item of interest (projectile, target or total system). The cg positions for the y and z axes are determined in a similar manner.

The three translational momenta ($M\bar{V}_x$, $M\bar{V}_y$, $M\bar{V}_z$) are obtained in a similar manner, with the momentum in the x direction given by

$$M\bar{V}_x = \sum M_i \dot{u}_i \qquad (53)$$

where $\dot{u}_i$ is the x velocity of node i and the summation again includes all nodes of the item of interest. If there are no external restraints in a particular direction, the translational momentum in that direction will remain unchanged for the total system.

The three rotational momenta (H_x, H_y, H_z) are obtained about the cg of the item of interest. The rotational momentum about the x axis is defined as

$$H_x = \sum M_i [\dot{w}_i(y_i - \bar{y}) - \dot{v}_i(z_i - \bar{z})] \tag{54}$$

where y_i and z_i are the coordinates of node i, and $\dot{v}_i$ and $\dot{w}_i$ are the corresponding velocities.

The kinetic energy is next determined from

$$KE = \frac{1}{2} \sum M_i (\dot{u}_i^2 + \dot{v}_i^2 + \dot{w}_i^2) \tag{55}$$

For the initial conditions it is assumed there is no internal energy which can be converted to kinetic energy. Therefore, the kinetic energy of the system cannot increase above its initial level. It can, however, decrease by being converted to various forms of internal energy.

The cg positions, momenta and kinetic energies are all parameters which are determined from the node variables. Various forms of internal energy are associated with the elements and are required for the determination of the temperature, T, in Equation (31) and the hydrostatic pressure, P, in Equation (32). The internal energy in an element is approximately determined from

$$E_s^{t+\Delta t} = E_s^t + [s_x \dot{e}_x + s_y \dot{e}_y + s_z \dot{e}_z + \tau_{xy} \dot{\gamma}_{xy} \tag{56}$$

$$+ \tau_{xz} \dot{\gamma}_{xz} + \tau_{yz} \dot{\gamma}_{yz} - (P + Q) \dot{\epsilon}_v] \Delta t$$

where $E_s^{t+\Delta t}$ is the internal energy per original unit volume at time $t+\Delta t$. The deviator stresses (s_x, s_y, s_z), shear stresses (τ_{xy}, τ_{xz}, τ_{yz}), hydrostatic pressure, and artificial viscosity (P,Q) are those obtained at time $t+\Delta t$. Likewise, the strain rates ($\dot{e}_x$, $\dot{e}_y$, $\dot{e}_z$, $\dot{\gamma}_{xy}$, $\dot{\gamma}_{xz}$, $\dot{\gamma}_{yz}$, $\dot{\epsilon}_v$) are for this same time. The time increment, Δt, is for the previous cycle between times t and

t+Δt. A more precise determination of the internal energy could be made by considering the stresses and strains at times t and t+Δt, but this would require a significant increase in storage requirements.

The total internal energy in an individual element at time, t, is $E_s^t V^O$, where V^O is the initial volume of the element. The total internal energy for the system is the sum of the internal energies of the individual elements. The total system energy is the sum of the system kinetic energy and the system internal energy, and it should be equal to the initial kinetic energy. A comparison of the total system energy with the initial kinetic energy gives an indication of the accuracy of the approximate formulation of Equation (56). This approximation is generally very accurate for high-velocity impact problems when the strains are constantly increasing. It may be less accurate, however, for problems where the strains are not constantly increasing. The effect of E_s in Equation (32) can be eliminated by setting the Grüneisen coefficient equal to zero.

The temperature of an element is obtained from the nonrecoverable work done on the element. When an element is in the plastic range, the work per original unit volume, E_w, is identical to that of Equation (56), except the effect of the hydrostatic pressure, P, is not included since its work can be recovered. The work done by the plastic and viscous deviator stresses, shear stresses and artificial viscosity cannot be recovered and, therefore, causes an increase in temperature. When the material is in the elastic range, only the work done by the artificial viscosity cannot be recovered. The temperature of an element is

$$ T = T_O + \frac{E_w}{C_s \rho^O} \tag{57} $$

where T_O is the initial temperature, C_s is the specific heat, and ρ^O is the initial density. The temperature only occurs in Equation (31), and its effect can be eliminated by setting $C_4 = 1.0$ and $C_5 = 0$.

2.8 SEVERE DISTORTIONS

It was previously stated that a tetrahedron element is well suited to represent severe distortions. In Reference 8 it is shown that a two-dimensional triangular element formulation is much better suited to represent severe distortions than is a formulation which uses a quadrilateral grid. This is due to a triangle's resistance to allowing a node to cross the opposite side of the triangle during high distortion. It is apparent that the cross-sectional area of a triangle approaches zero as a node approaches the opposite side of that triangle. Since the hydrostatic pressure is inversely proportional to the volume of the element, as the volume approaches zero, the pressure approaches infinity. As a result, there is a very large resistance to this mode of distortion, and the triangle will not go through a zero-volume configuration, provided the time increment is properly controlled.

The quadrilateral formulation does not have this desirable characteristic. Figure 5 shows three quadrilateral configurations which have equal cross-sectional areas, A_o. Configuration A shows a rectangular cross section with nodes i, j, m and p defining the initial geometry. Configuration B represents a deformed element, with nodes j and m occupying the same position. A triangular element with two nodes occupying the same position would result in a zero cross-sectional area. For the quadrilateral element, however, nodes i and p can be displaced to allow the initial area to be retained. Configuration C shows overlapping nodes, and the net area of the quadrilateral is equal to the difference of the two triangular cross sections. Even this configuration can exist with the initial area. When this type of distortion is achieved, however, the formulation generally breaks down, and numerical instability often occurs. The deformations represented by configurations B and C usually occur when the grid is highly distorted. These deformations are resisted by the deviator and shear stresses, but these stresses are limited by the strength of the material and do not provide the potential magnitude of resistance as does the hydrostatic pressure for the triangular elements.

28
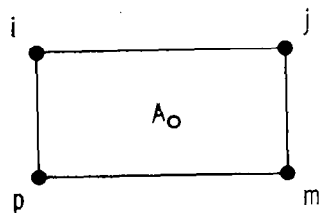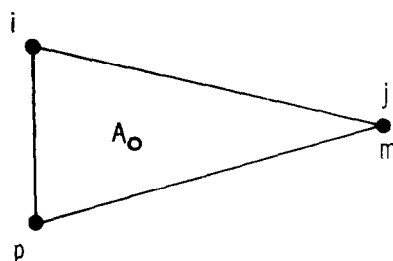
CONFIGURATION A

CONFIGURATION B
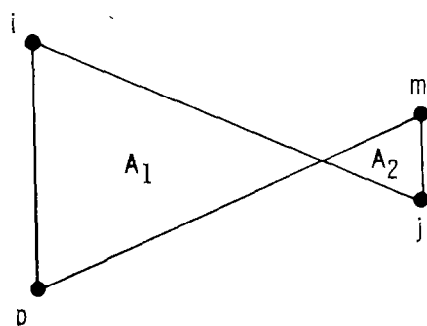
CONFIGURATION C

$$A_o = A_1 - A_2$$

Figure 5. Possible Distortions of a Quadrilateral Element

The three-dimensional tetrahedron element used in the EPIC-3 code is analagous to the two-dimensional triangular element with respect to severe distortions. The lines connecting the nodes cannot become tangled or overlapped since the tetrahedron must also go through a zero-volume configuration (and therefore infinite pressure) before this can occur. This is not the case for any three-dimensional element with more than four sides. Since many impact problems produce severe distortions, this is a very important feature of the tetrahedron element formulation.

2.9 EXAMPLE

An example problem is shown in Figure 6 to illustrate the EPIC-3 computational technique. It involves oblique impact (60 degrees from normal) of a steel sphere onto an aluminum plate at 729 m/s. The sphere diameter and plate thickness are both equal to 0.635 cm. The yield and ultimate stresses are taken to be the static values of 2.07 and 2.28 GPa for the steel sphere, and 0.31 and 0.45 GPa for the aluminum plate. This problem was selected because test data in Reference 9 indicate the sphere should ricochet off the surface of the plate.

The initial geometry in Figure 6 is defined by 831 nodes and 3192 tetrahedron elements. Note that the geometry of the sphere can be adequately represented with the tetrahedron elements. The outer nodes of the sphere are the slave nodes, and the nodes on the top surface of the plate are the master nodes as shown in Figure 3. The deformed shape at 12 μs after impact is shown, and this is the time at which the vertical component of the sphere velocity is equal to zero. Thereafter, the sphere moves upward, away from the plate. At 40 μs after impact, the sphere has separated from the plate and is flying freely. This problem required 507 cycles of integration and slightly less than three hours of central processor time on a Honeywell 6080 computer.

729 M/S

1.0 CM

STEEL SPHERE→

FINITE ELEMENT MODEL

ALUMINUM
PLATE

12 μS AFTER IMPACT

40 μS AFTER IMPACT
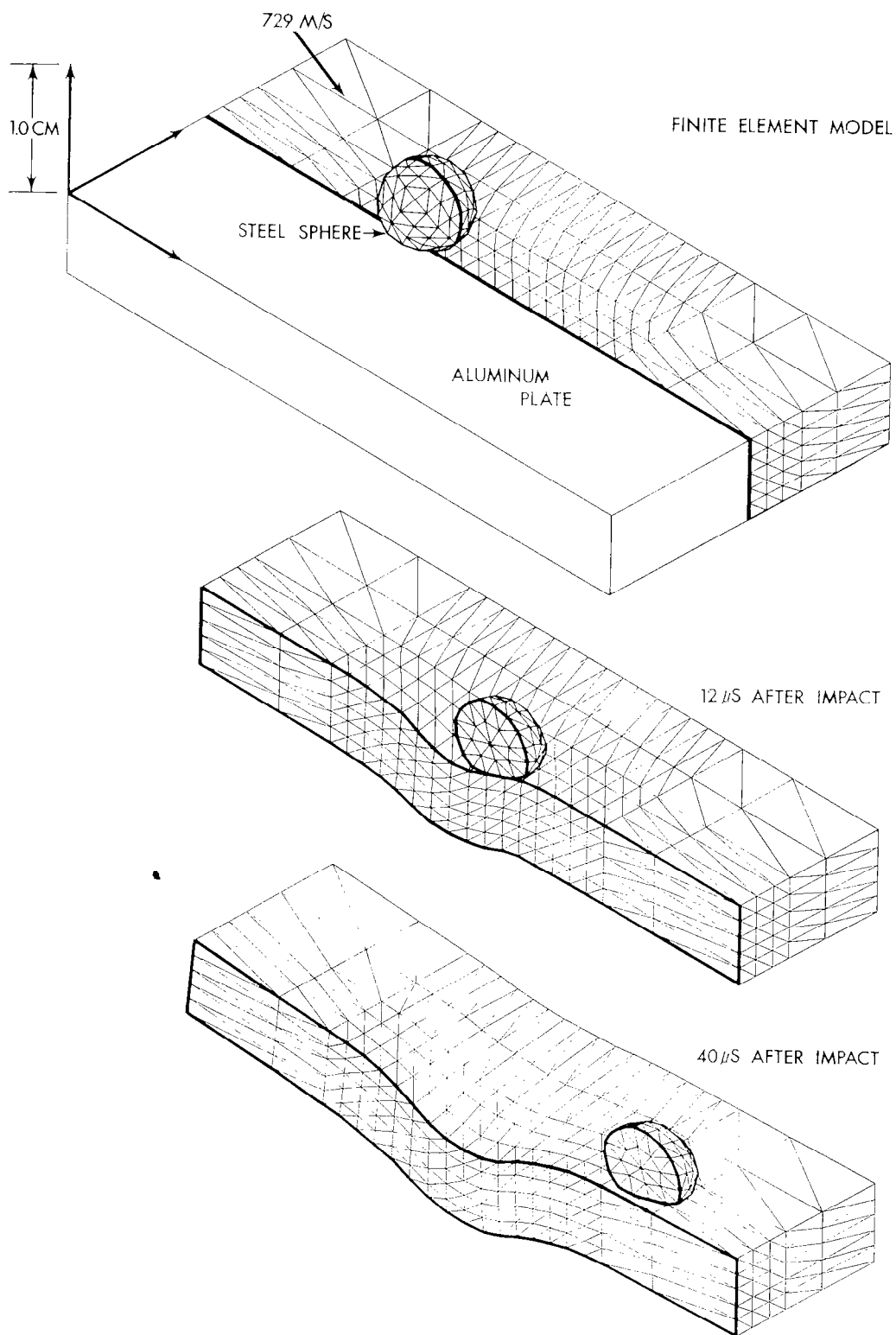
Figure 6. Oblique Impact (60 degrees from normal) of a Steel
Sphere onto an Aluminum Plate at 729 m/s

31

The cross-section of the plate at 40 μs is in good general agreement with the test data reported in Reference 9. It is anticipated that there would be even better agreement if the finite-element model were extended in the horizontal directions to represent a larger plate, if a finer network of nodes were used, and if dynamic material properties were used in place of the static material properties.

It was previously mentioned that slight errors in rotational momenta and cg positions can result with this formulation. Since the initial path of the sphere does not pass through the cg of the plate, the initial system (sphere and plate) has a rotational momentum about the axis normal to the plane of symmetry. At 40 μs after impact, when the sphere is flying freely, this rotational momentum is within 1 percent of the initial value. The cg errors associated with the rigid-body translation of the system are significantly less than 1 percent. There are no errors in the translational momenta since these parameters are conserved in the basic formulation.

Additional examples, involving wave propagation, severe distortions and material fracture, are provided in References 10 and 11.

SECTION III

COMPUTER PROGRAM DESCRIPTION

The EPIC-3 computer program contains the formulation presented in Section II. A description of some of the characteristics of the computer program is given in the following subsections.

3.1 PROGRAM ORGANIZATION AND SUBROUTINES

The organization of the EPIC-3 code is shown in Figure 7. It consists of the main program, EPIC-3, and 21 subroutines for a total of 4344 cards. A plotting program is also available to give two-dimensional plots of the x-z plane at y = 0 (plane of symmetry). The following is a brief description of the main program and subroutines (listed alphabetically) shown in Figure 7.

EPIC-3   This is the main program which calls subroutines MATL, GEOM, START and LOOP. For restart calculation, the program goes directly to subroutine LOOP (56 cards).

BREAK   This subroutine checks for fracture (20 cards).

BRICK   This subroutine generates a series of composite brick elements, each composed of six tetrahedron elements (A, B, C, D, E, F) as shown in Figure 8 (49 cards).

DETERM   This subroutine calculates the determinate of an array for volume calculations (50 cards).
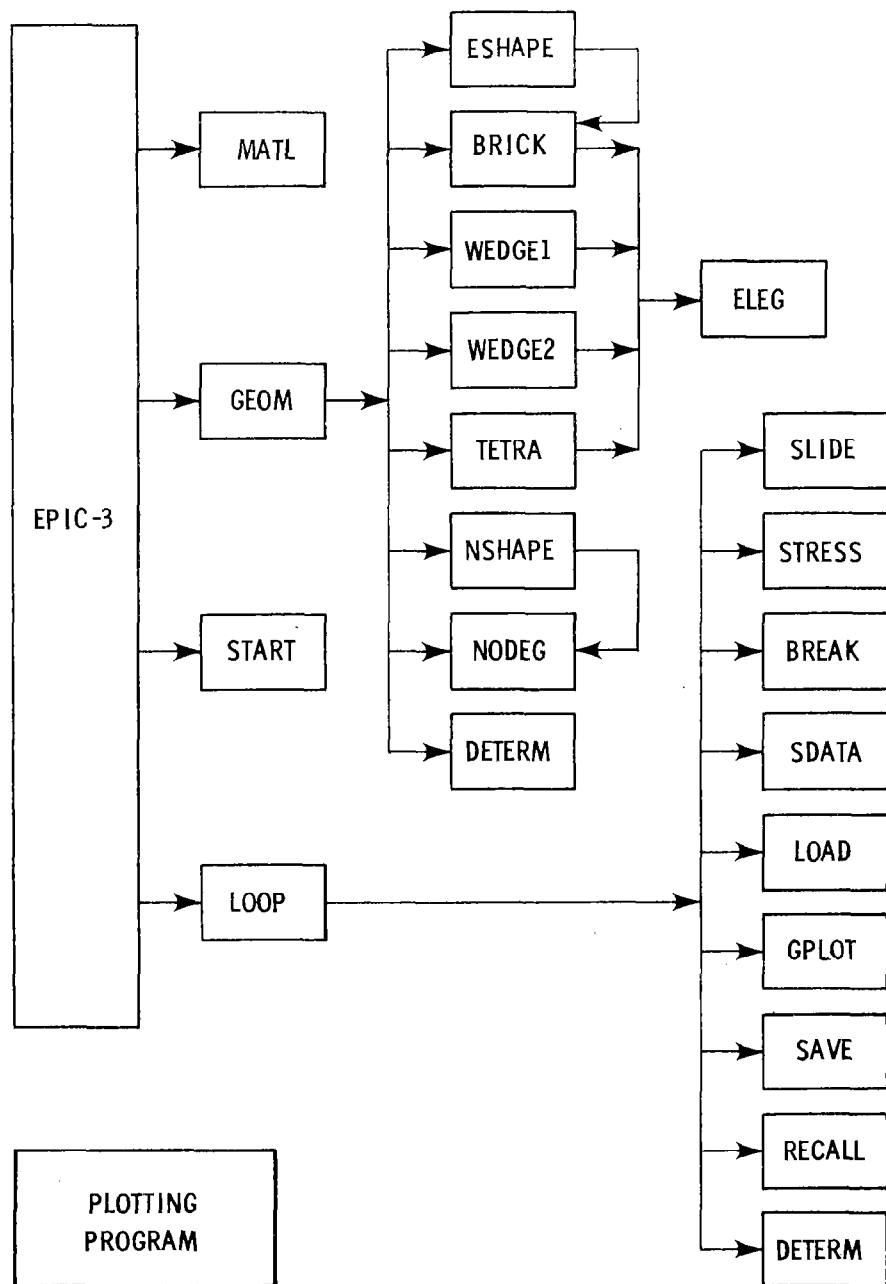
Figure 7. EPIC-3 Program Subroutine Arrangement
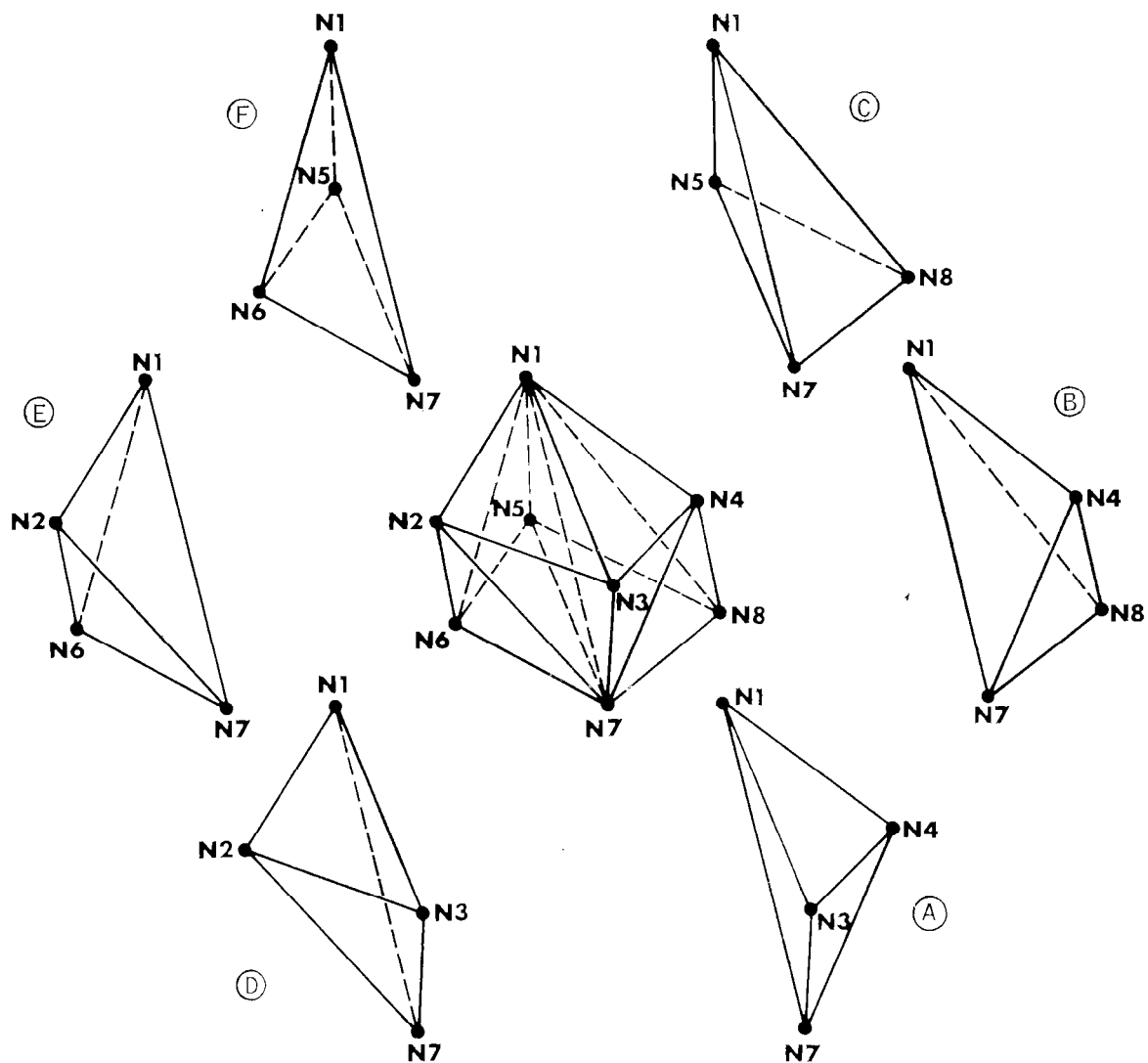
Figure 8. Arrangement of Six Tetrahedra into
a Composite Brick Element

ELEG   This subroutine generates data for a single tetrahedron element
            and places this initial data into the appropriate internal file
            (43 cards).

ESHAPE   This subroutine generates elements for various special shapes
            composed of rod geometry, rounded-nose geometry, conical-
            nose geometry and flat-plate geometry (1269 cards).

GEOM   This subroutine reads, generates and prints the initial
            geometry (451 cards).

GPLOT   This subroutine writes data on Tape3 for geometry plots
            (52 cards).

LOAD   This subroutine calculates axial forces, shear forces and
            bending moments in a slender projectile (69 cards).

LOOP   This subroutine calculates the equations of motion, strains,
            strain rates, stresses and concentrated nodal forces. It
            also prints selected node and element data (520 cards).

MATL   This subroutine reads, calculates and prints the material
            properties (156 cards).

NODEG   This subroutine generates a row of nodes (69 cards).

NSHAPE   This subroutine generates nodal geometry for various
            special shapes composed of rod geometry, rounded-nose
            geometry, conical-nose geometry and flat-plate geometry
            (581 cards).

RECALL   This subroutine reads data from Tape2 for a restart run
            (88 cards).

SAVE   This subroutine writes data on Tape2 for a restart run (76 cards).

SDATA   This subroutine calculates, prints and saves (Tape4) system data such as cg positions, kinetic energies, and linear and angular momenta for the projectile, target and total system (229 cards).

SLIDE   This subroutine calculates the equations of motion of the slave nodes. If there is interference, it places the slave node on the master surface and transfers the lost momenta of the slave nodes to the appropriate master nodes (256 cards).

START   This subroutine reads the initial dynamic conditions and sets the variables equal to the conditions which exist at impact (108 cards).

STRESS   This subroutine calculates element stresses which consist of elastic stresses, plastic and viscous deviator stresses, hydrostatic pressure and artificial viscosity (89 cards).

TETRA   This subroutine generates a series of tetrahedron elements (33 cards).

WEDGE1   This subroutine generates a series of composite wedge elements, each composed of three tetrahedron elements containing nodes N1, N3, N4, N5, N7, N8, (Elements A, B, C), as shown in Figure 8 (40 cards).

WEDGE2   This subroutine generates a series of composite wedge elements, each composed of three tetrahedron elements containing nodes N1, N2, N3, N5, N6, N7, (Elements D, E, F), as shown in Figure 8 (40 cards).

The plotting program reads from Tape3 (written by subroutine GPLOT) and generates a two-dimensional, cross-sectional plot of the x-z plane at y = 0.

3.2 PROGRAM LOGIC AND STORAGE ALLOCATIONS

Program logic and storage allocation are shown schematically in Figure 9. The existing EPIC-3 code is dimensioned for a maximum of 2000 nodes, as shown. The element data are stored on two disk files in blocks of 200 elements each. Since only one block of element data is in core at any specific time, there is no limit to the number of elements. Relatively small storage allocations are made for material properties and sliding-surface data which identify the master nodes and slave nodes. The EPIC-3 code, with a capacity of 2000 nodes, requires 69K storage in a Honeywell 6080 computer. There are generally about four to five times as many elements as nodes, so this version of the program could provide solutions for problems involving up to 2000 nodes and about 10,000 elements. It should also be noted that many computers (including the Honeywell 6080) have storage capacities significantly greater than 69K. Therefore, by increasing the dimensions of the node arrays, solutions to much larger problems can be obtained with the existing code.

Most of the computations occur in two large loops, the node loop and the element loop. The primary activity for the node loop is to apply the equations of motion to all nodes using the updated accelerations from the concentrated forces which were accumulated during the previous element loop.

The element loop operates on each element in a consecutive order beginning with the first element in the first block, and ending with the last element in the last block. The important activities in the element loop are:

38
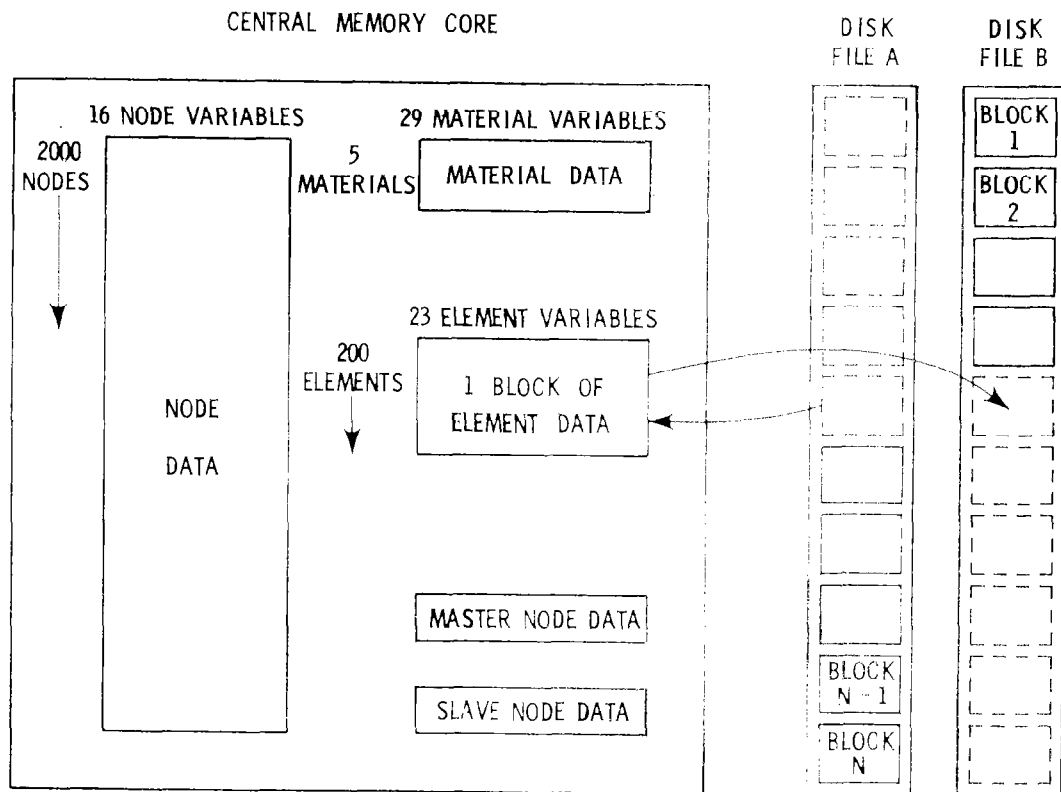
Figure 9. EPIC-3 Program Logic and Storage

- Bring block of element data from File A when computations on previous block are complete.

- Obtain updated element data such as strains and strain rates. Since the strains and strain rates are dependent on the current displacements and velocities of the nodes, pointers are required to obtain these data from the node arrays which are always in the central memory core.

- Obtain stresses in the elements using the updated strains and strain rates. This activity requires a pointer to the material arrays.

- Calculate the concentrated nodal forces from the updated stresses, and distribute them to the appropriate node arrays with the same pointers used to obtain the displacements and velocities.

- When the entire block of element data has been processed, write the updated data on File B and bring the next block of element data into core.

It should be noted that all blocks (and therefore all elements) are processed before the next node loop begins. Also, for the element loop computations during the next integration time increment, disk Files A and B are interchanged.

3.3 NODE AND ELEMENT ARRAYS

There are 16 node variables which are contained in arrays and 23 element variables contained in arrays as shown in Figure 9. The node arrays are described as follows:

NODE   Identifies the node number such that it is not necessary to have a consecutive node numbering system

AMASS   The total mass of the node

PMASS   The mass of the node contributed by the projectile

XI   The initial x coordinate of the node

YI   The initial y coordinate of the node

ZI   The initial z coordinate of the node

X	The displaced x coordinate of the node
Y	The displaced y coordinate of the node
Z	The displaced z coordinate of the node
XDOT	The x velocity of the node
YDOT	The y velocity of the node
ZDOT	The z velocity of the node
PX	The x direction concentrated force on the node
PY	The y direction concentrated force on the node
PZ	The z direction concentrated force on the node
IFIX	Identifies X, Y, Z restraints on the node. It also identifies a slave node and indicates if it is free or sliding on the master surface.

The element arrays are described as follows:

NEL	Identifies the element number
NODE 1	Node number of node i (see Figure 2)
NODE 2	Node number of node j
NODE 3	Node number of node m

NODE 4	Node number of node p
MAT	Material number
BI	
BJ	
BM	
BP	
CI	
CJ	Initial geometry-dependent constants defined in Equations (6c) through (6e).
CM	
CP	
DI	
DJ	
DM	
DP	
VOL	Initial volume
DVOL	Volumetric strain defined in Equation (13)
ES	Total internal energy per original unit volume defined in Equation (56)
EW	Heat energy per original unit volume
ICHECK	Identifies state of material (elastic, plastic, fractured)

SECTION IV
PROGRAM USER INSTRUCTIONS

The required EPIC-3 input data for various conditions are summarized in Figure 10 and described in subsections 4.1 through 4.4. Output data are described in subsection 4.5. Succeeding subsections deal with diagnostics, estimated central processor time requirements, and central memory storage requirements and alterations.

4.1 INPUT DATA FOR AN INITIAL RUN

An initial run is one which requires input data for the initial geometry and impact conditions at time = 0. The descriptions which follow are for the input data in Figure 10. Consistent units must be used.

- **Identification Card (2I5, F10. 0)** -

    CASE   =   Case number for run identification

    CYCLE =   0 for initial run

    CPMAX =   Central Processor time (hours) at which the results will be written into the restart tape and the run will stop. This feature will be bypassed if CPMAX = 0.

- **24 Material Cards (5E15. 8)** - Each of the 24 material cards provides a specific material characteristic for five materials. For instance, the first card describes the density of the materials. The density of material 1 is entered in columns 1-15, the density of material 2 in columns 16-30, etc. The second card contains the specific heats for the five materials, etc. It is only necessary to describe the materials used for the analysis. If materials 1 and 3 are used for a specific

43

INITIAL RUN INPUT DATA

IDENTIFICATION CARD (2I5, F10.0)

CASE	CYCLE	CPMAX	

24 MATERIAL CARDS (5E15.8)

MATL1	MATL2	MATL3	MATL4	MATL5	

PROJECTILE SCALE / SHIFT / ROTATE CARD (6F10.0)

XSCALE	YSCALE	ZSCALE	XSHIFT	ZSHIFT	ROTATE	

PROJECTILE NODE DATA CARDS - AS REQUIRED (3I5, 2X, 3I1, 7F8.0)

N1	NN	INC		X1	Y1	Z1	XN	YN	ZN	EXPAND	

└─IX, IY, IZ

BLANK CARD

PROJECTILE NODE SPECIAL SHAPES - AS REQUIRED (DESCRIPTION FOLLOWS)

BLANK CARD

TARGET SCALE / SHIFT / ROTATE CARD (6F10.0)

XSCALE	YSCALE	ZSCALE	XSHIFT	ZSHIFT	ROTATE	

TARGET NODE DATA CARDS - AS REQUIRED (3I5, 2X, 3I1, 7F8.0)

N1	NN	INC		X1	Y1	Z1	XN	YN	ZN	EXPAND	

└─IX, IY, IZ

BLANK CARD

TARGET NODE SPECIAL SHAPES - AS REQUIRED (DESCRIPTION FOLLOWS)

BLANK CARD

PROJECTILE ELEMENT DATA CARDS - AS REQUIRED (13I5)

ELE1	ELEN	ELE INC	MATL	N1	N2	N3	N4	N5	N6	N7	N8	NODE INC	

BLANK CARD

PROJECTILE ELEMENT SPECIAL SHAPES - AS REQUIRED (DESCRIPTION FOLLOWS)

BLANK CARD

Figure 10.   EPIC-3 Input Data Summary
(1 of 3)

44

TARGET ELEMENT DATA CARDS - AS REQUIRED (13I5)

ELE1	ELEN	ELE INC	MATL	N1	N2	N3	N4	N5	N6	N7	N8	NODE INC	

BLANK CARD

TARGET ELEMENT SPECIAL SHAPES - AS REQUIRED (DESCRIPTION FOLLOWS)

BLANK CARD

SLIDE / LOAD CARD (5I5)

NSLID	IRIG	NTOP	NBOT	NRING	

SLIDING SURFACE IDENTIFICATION CARDS - AS REQUIRED (4I5)

TYPE	NMX	NMY	NSLAV	

MASTER NODES - AS REQUIRED (16I5) NMY ROWS WITH NMX NODES PER ROW

START EACH ROW WITH NEW CARD

IM1	IM2													IM15	IM16

SLAVE NODES - AS REQUIRED (16I5)

IS1	IS2													IS15	IS16

INITIAL VELOCITY CARD (6F10.0)

PXDOT	PYDOT	PZDOT	TXDOT	TYDOT	TZDOT	

INTEGRATION TIME INCREMENT CARD (5F10.0)

DT1	DTMAX	DTMIN	STF	TMAX	

DATA OUTPUT CARDS - AS REQUIRED (2F10.0, 4I5)

TIME	ECHECK	ISYS	ILOAD	ISAVE	IPLOT	

RESTART RUN INPUT DATA

IDENTIFICATION CARD (2I5, F10.0)

CASE	CYCLE	CPMAX	

INTEGRATION TIME INCREMENT CARD (3F10.0)

DTMIN	STF	TMAX	

DATA OUTPUT CARDS - AS REQUIRED (2F10.0, 4I5)

TIME	ECHECK	ISYS	ILOAD	ISAVE	IPLOT	

Figure 10. EPIC-3 Input Data Summary
(2 of 3)

SPECIAL SHAPES INPUT DATA

3 NODE CARDS FOR EACH ROD SHAPE (4I5, 3F10.0 / 5F10.0 / 5F10.0)

1	N1	NRING	NPLN	ZTOP	ZBOT	EXPAND	

RTOP1	RTOP2	RTOP3	RTOP4	RTOP5	

RBOT1	RBOT2	RBOT3	RBOT4	RBOT5	

3 NODE CARDS FOR EACH NOSE SHAPE (3I5, 5X, F10.0 / 5F10.0 / 5F10.0)

        INOSE = 2 →ROUNDED NOSE,   INOSE = 3 →CONICAL NOSE

INOSE	N1	NRING		ZTOP	

RTOP1	RTOP2	RTOP3	RTOP4	RTOP5	

ZMIN1	ZMIN2	ZMIN3	ZMIN4	ZMIN5	

3 NODE CARDS FOR EACH FLAT PLATE SHAPE (2I5 / 6I5, 3F10.0 / 6F10.0)

4	N1	

NX	NY	NZ	IDY	IDZ	IY	X-EXPAND	Y-EXPAND	Z-EXPAND	

X1	Y1	Z1	XN	YN	ZN	

ELEMENT CARD FOR EACH ROD SHAPE (10I5)

1	N1	NRING	NLAY	ELE1	M1	M2	M3	M4	M5	

ELEMENT CARD FOR EACH NOSE SHAPE (3I5, 5X, 6I5)

        INOSE = 2 →ROUNDED NOSE,   INOSE = 3 →CONICAL NOSE

INOSE	N1	NRING		ELE1	M1	M2	M3	M4	M5	

ELEMENT CARD FOR EACH FLAT PLATE SHAPE (3I5, 5X, 5I5)

4	N1	4		ELE1	MATL	NLX	NLY	NLZ	

Figure 10. EPIC-3 Input Data Summary
(3 of 3)

analysis, all the material 1 data must be specified in columns 1-15 and all the material 3 data in columns 31-45. Columns 16-30, 46-60, and 61-75, representing materials 2, 4 and 5, can be left blank.

Card 1   Density (mass/volume)

Card 2   Specific heat (work/mass/degree)

Card 3   Modulus of elasticity (force/area)

Card 4   Poisson's ratio

Card 5   Absolute viscosity (force-time/area)

Card 6   Yield stress (force/area)

Card 7   Ultimate stress (force/area)

Card 8   Strain at which the ultimate stress is achieved. Should be consistent with the strain definition in Equation (14). Stress varies linearly between the strain at the yield stress and the strain at the ultimate stress.

The stress for larger strains is equal to the ultimate stress until fracture occurs.

Card 9   Maximum negative hydrostatic pressure (force/area)

Card 10   Strain rate effect constant, C_1, in Equation (31)

Card 11   Pressure effect constant, C_2, in Equation (31)

Card 12   Pressure effect constant, C_3, in Equation (31)

Card 13   Temperature effect constant, C_4, in Equation (31)

Card 14   Temperature effect constant, C_5, in Equation (31)

Card 15   Hydrostatic pressure constant, K_1, in Equation (32) (force/area)

Card 16   Hydrostatic pressure constant, K_2, in Equation (32) (force/area)

Card 17   Hydrostatic pressure constant, K_3, in Equation (32)
           (force/area)

Card 18   Grüneisen coefficient, Γ, in Equation (32)

Card 19   Linear artificial viscosity coefficient, C_L, in Equation (33)

Card 20   Quadratic artifical viscosity coefficient, C_O^2, in Equation (33)

Card 21   Equivalent strain ⎫ if both are exceeded, the element is totally

Card 22   Volumetric strain ⎭ failed and produces no stresses or pressures.

Card 23   Equivalent strain for shear and tensile failure only. Positive
           hydrostatic pressure and viscosity stress capability remain.
           If negative, the material behaves like a liquid.

Card 24   Initial temperature (degrees)

● Projectile Scale/Shift/Rotate Card (6F10. 0) -

XSCALE   =   Factor by which the x coordinates of all projectile
               nodes are multiplied. Applied after the coordinate
               shifts (XSHIFT, ZSHIFT) described later.

YSCALE   =   Factor by which the y coordinates are multiplied.

ZSCALE   =   Factor by which the z coordinates are multiplied.

XSHIFT   =   Increment added to the x coordinates of all projectile
               nodes (length). Applied before the scale factors
               (XSCALE, YSCALE, ZSCALE).

ZSHIFT   =   Increment added to the z coordinates (length).

ROTATE   =   Rotation about the y axis (at x=z=0) of all projectile
               nodes (degrees). Applied after the coordinate shifts
               (XSHIFT, ZSHIFT), and the scale factors (XSCALE,
               YSCALE, ZSCALE).

48

- Projectile Node Data Cards (3I5, 2X, 3I1, 7F8.0) - The projectile node data cards are provided as required for the projectile nodes. If a node is at the interface of the projectile and the target, and contains mass from both the projectile and the target, it must be included with the projectile nodes. The node numbers (N1··· NN) must not exceed the dimension of the node arrays, and they need not be numbered consecutively or in increasing order. End with a blank card.

N1	=	First node in a row of nodes.
NN	=	Last node in a row of nodes. Leave blank if a single node (not a row) is entered.
INC	=	Node number increment between adjacent nodes. If left blank, program will set INC = 1.
IX	=	1 will restrain all nodes (N1··· NN) in the x direction. No restraint if left blank.
IY	=	1 will restrain nodes in y direction.
IZ	=	1 will restrain nodes in z direction
X1	=	x coordinate of node N1 (length)
Y1	=	y coordinate of node N1 (length)
Z1	=	z coordinate of node N1 (length)
XN	=	x coordinate of node NN (length). Leave blank if a single node is entered.
YN	=	y coordinate of node NN (length)
ZN	=	z coordinate of node NN (length)
EXPAND	=	Factor by which the distance between adjacent nodes changes. For example, if the distance between the first two nodes is Δ_1, the distance between the second and third nodes is $\Delta_2 = \Delta_1 \cdot$ EXPAND. A summary of

relative spacing between the first two nodes and the
last two nodes is given in Figure 11. If left blank,
the program will set EXPAND = 1.0 for uniform
spacing.

- Projectile Node Special Shapes - These are described later. End with
a blank card.

- Target Scale/Shift/Rotate Card (6F10.0) - Same as Projectile Scale/
Shift/Rotate Card except it applies to the target nodes.

- Target Node Data Cards (3I5, 2X, 3I1, 78F.0) - Same as Projectile Node
Data Cards except these apply to the target nodes. If there are inter-
face nodes which contain mass from both the projectile and the target,
these nodes are included with the projectile nodes and must not be
included here. End with a blank card.

- Target Node Special Shapes - These are described later. End with a
blank card.

- Projectile Element Data Cards (13I5) - The Projectile Element Data
Cards are provided as required for the projectile elements. For this
immediate discussion it will be assumed that the elements are entered
as a series of composite brick elements, each containing six individual
elements as shown in Figure 8. Following this immediate discussion
will be an example and instructions for generating a series of
individual elements. End with a blank card.

ELE1　　　=　　First individual element in the first composite brick
element in a series of composite brick elements.
The six elements in a composite brick element are
numbered consecutively.

50

EXPAND

NUMBER OF INCRE-MENTS N	.7		.8		.9		1.0		1.1		1.2		1.3		1.4		1.5	
	$\frac{\Delta_1}{\bar{\Delta}}$	$\frac{\Delta_N}{\bar{\Delta}}$	$\frac{\Delta_1}{\bar{\Delta}}$	$\frac{\Delta_N}{\bar{\Delta}}$	$\frac{\Delta_1}{\bar{\Delta}}$	$\frac{\Delta_N}{\bar{\Delta}}$	$\frac{\Delta_1}{\bar{\Delta}}$	$\frac{\Delta_N}{\bar{\Delta}}$	$\frac{\Delta_1}{\bar{\Delta}}$	$\frac{\Delta_N}{\bar{\Delta}}$	$\frac{\Delta_1}{\bar{\Delta}}$	$\frac{\Delta_N}{\bar{\Delta}}$	$\frac{\Delta_1}{\bar{\Delta}}$	$\frac{\Delta_N}{\bar{\Delta}}$	$\frac{\Delta_1}{\bar{\Delta}}$	$\frac{\Delta_N}{\bar{\Delta}}$	$\frac{\Delta_1}{\bar{\Delta}}$	$\frac{\Delta_N}{\bar{\Delta}}$
2	1.176	.824	1.111	.889	1.053	.947	1.0	1.0	.952	1.048	.909	1.091	.870	1.130	.833	1.167	.800	1.200
3	1.370	.671	1.230	.787	1.107	.897			.906	1.097	.824	1.187	.752	1.271	.688	1.349	.632	1.421
4	1.579	.542	1.355	.694	1.163	.848			.862	1.147	.745	1.288	.647	1.420	.563	1.545	.492	1.662
5	1.803	.433	1.487	.609	1.221	.801			.819	1.199	.672	1.393	.553	1.579	.457	1.755	.379	1.919
6	2.040	.343	1.626	.533	1.281	.756			.778	1.252	.604	1.504	.470	1.746	.368	1.977	.289	2.192
7	2.288	.269	1.772	.464	1.342	.713			.738	1.307	.542	1.618	.398	1.922	.293	2.210	.218	2.487
8	2.547	.210	1.923	.403	1.405	.672			.700	1.363	.485	1.737	.335	2.104	.233	2.452	.162	2.775
9	2.814	.162	2.079	.349	1.469	.632			.663	1.421	.433	1.861	.281	2.293	.183	2.702	.120	3.080
10	3.087	.125	2.241	.301	1.535	.595			.627	1.479	.385	1.988	.235	2.488	.143	2.959	.088	3.392
12	3.651	.072	2.577	.221	1.672	.525			.561	1.601	.303	2.253	.161	2.893	.086	3.490	.047	4.031
14	4.229	.041	2.929	.161	1.815	.461			.500	1.728	.237	2.530	.109	3.315	.051	4.036	.024	4.683
16	4.816	.023	3.293	.116	1.964	.404			.445	1.859	.183	2.819	.073	3.749	.030	4.592	.012	5.341
18	5.409	.013	3.666	.083	2.118	.353			.395	1.995	.140	3.117	.048	4.191	.017	5.155	.006	6.004
20	6.003	.005	4.037	.046	2.246	.273			.312	2.102	.089	3.407	.024	4.634	.007	5.719	.002	6.668

NODES   N1   (N1 + INC)   (NN – INC)   NN

INCREMENTS Δ_1 Δ_2 Δ_{I-1} Δ_I Δ_{I+1} Δ_{N-1} Δ_N
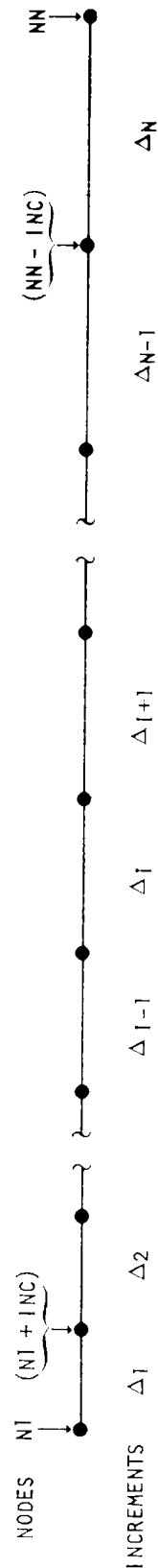
$\bar{\Delta} = \dfrac{\text{TOTAL LENGTH}}{\text{NUMBER INCREMENTS}} = \dfrac{L}{N}$

$\Delta_{I+1} = \Delta_I \cdot \text{EXPAND}$

Figure 11. Nodal Spacing for Various Expansion Factors

51

ELEN   =   First individual element in the last composite brick
                 element in a series of composite brick elements.
                 Note that this is the first, rather than last, individual
                 element in the last composite brick element.   Leave
                 blank if a single composite element is entered.

ELE INC   =   Element number increment between the first individual
                 element of successive composite brick elements.
                 Since each composite brick element contains six indivi-
                 dual elements, this increment must not be less than six.
                 If left blank the program will set ELE INC = 6.

MATL   =   Material number (1, 2, 3, 4, or 5) of the elements.   If
                 left blank, the material number from the previous ele-
                 ment data card will be used.

N1 - N8   =   Node numbers of the first composite brick element as
                 shown in Figure 8.   Nodes N1, N2, N3 and N4, and
                 nodes N5, N6, N7 and N8, are counterclockwise when
                 looking from N1 to N5.

NODE INC   =   The node number increment added to the node numbers
                 of the previous composite brick element for the next
                 composite brick element.   If left blank, the program
                 will set NODE INC = 1.

An example of input data for composite brick elements is shown in
Figure 12.   In the upper left corner it can be seen that there are four
rows of nodes (12-18, 22-28, 32-38, 42-48) which are arranged to
contain three composite brick elements.   If ELE1 = 101, ELEN = 121
and ELE INC = 10, then the first composite brick contains elements
101-106, the second contains 111-116, and the third contains 121-126.
The first composite brick is defined by nodes N1 = 12, N2 = 22, N3 = 32,
N4 = 42, N5 = 14, N6 = 24, N7 = 34 and N8 = 44.   Note that N1-N4 and
N5-N8 are counterclockwise when looking from N1 to N5.   The six
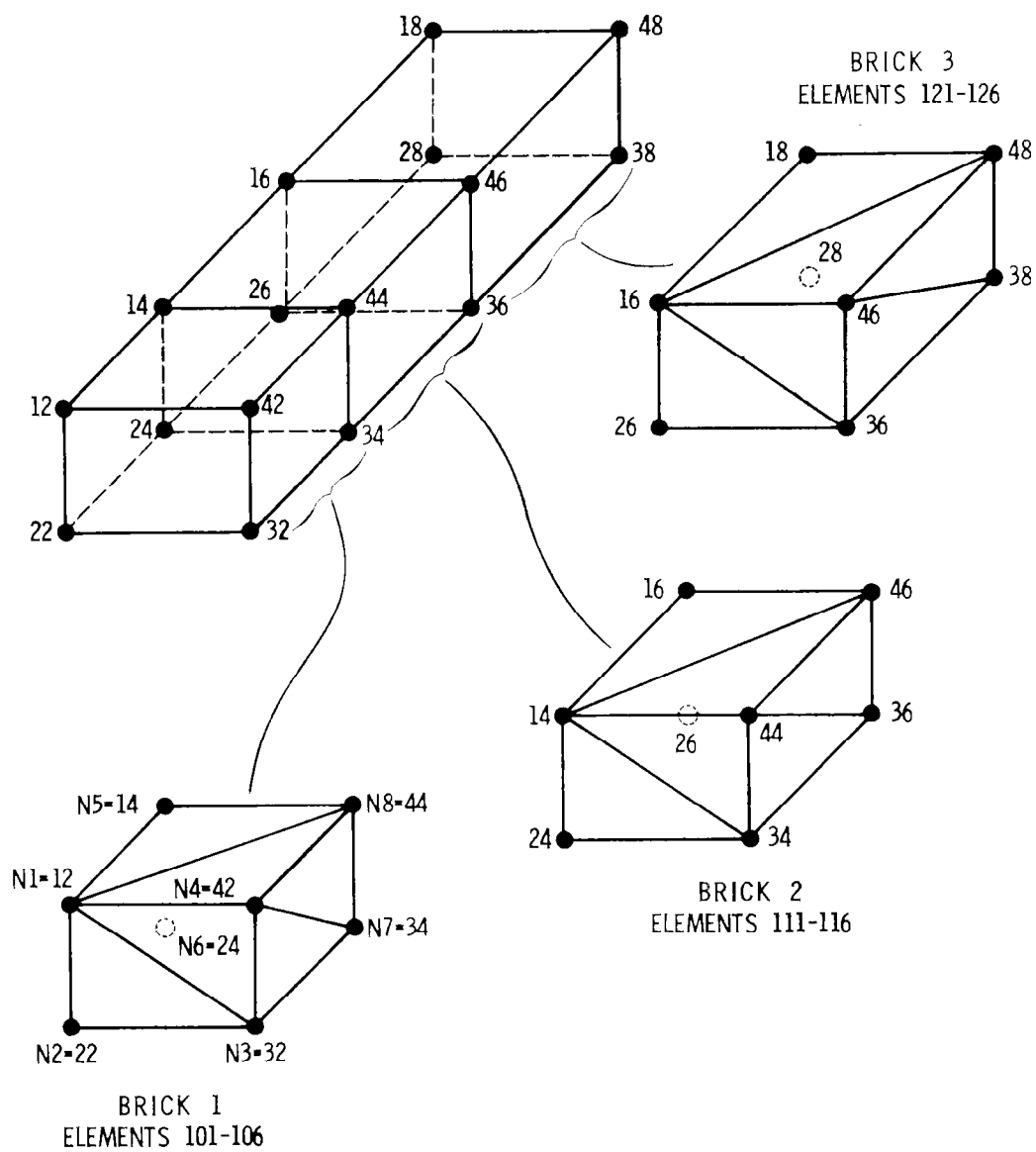
Figure 12. Node-Element Input Data Example

individual elements are generated according to the arrangement and order (A, B, C, D, E, F) shown in Figure 8. The node numbers for each successive brick are simply NODE INC = 2 greater than those of previous brick. For the second brick for instance, N1 = 12 + 2 = 14, N2 = 22 + 2 = 24, N3 = 32 + 2 = 34, N4 = 42 + 2 = 44, N5 = 14 + 2 = 16, N6 = 24 + 2 = 26, N7 = 34 + 2 = 36 and N8 = 44 + 2 = 46.

It is possible to generate a series of individual tetrahedron elements by letting N1-N4 be the nodes of the first element, where N1, N2, and N3 are counterclockwise when viewed from N4. This option is exercised when N5-N8 are left blank. For this option, if ELE INC is left blank, the program will set ELE INC = 1. It is also possible to generate a series of composite wedge elements, each containing three individual tetrahedron elements. The three elements in a composite wedge element are numbered consecutively. If N2 and N6 are left blank, the first three tetrahedron elements (A, B, C) are defined by nodes N1, N3, N4, N5, N7 and N8 as shown in Figure 8. Likewise, if N4 and N8 are left blank, the first three elements (D, E, F) are defined by nodes N1, N2, N3, N5, N6 and N7. For the composite wedge element options, if ELE INC is left blank, the program sets ELE INC = 3, which is the minimum acceptable increment.

- Projectile Element Special Shapes - These are defined later. End with a blank card.

- Target Element Data Cards (13I5) - Same as Projectile Element Data Cards. End with a blank card.

- Target Element Special Shapes - These are defined later. End with a blank card.

- Slide/Load Card (5I5) -

  NSLID =   The number of sliding surfaces. Currently limited to a maximum of two. This does not include the rigid sliding surface described next.

IRIG   =   1 gives a rigid frictionless surface on the positive side of the plane described by z = 0. If the equations of motion cause a node to have a negative z coordinate, the node coordinate is redefined and set at z = 0. If IRIG = 0 this option is not used.

The next three variables (NTOP, NBOT, NRING) are used to identify the nodal geometry for internal load calculations in a slender projectile. If this option is used, the nodal geometry must be consistent with the arrangement of nodes generated by the special shapes generator for rod geometry. Leave blank if it will not be used.

NTOP   =   The node number of the centerline node at the top free end of the cylindrical projectile.

NBOT   =   The node number of the centerline node at the lower end of the cylindrical portion of the projectile.

NRING   =   The number of rings of elements in the cylindrical projectile. This will be described in the discussion of special shapes.

- Sliding Surface Identification Cards (4I5) – Each sliding surface contains one identification card and cards (as required) describing the master nodes and the slave nodes. If there are no sliding surfaces (NSLID = 0), the Initial Velocity Card (described later) follows the previously described Slide/Load Card. If there are two sliding surfaces, the Sliding Surface Identification Card for the second sliding surface follows the slave node data for the first sliding surface.

TYPE   =   1 gives the slave surface above the master surface relative to the z axis. TYPE = 2 gives slave surface below the master surface relative to the z axis. In both cases the z coordinates of the master surface must be a single-valued function of x and y as discussed in subsection 2.6.

55

- <u>Data Output Cards (2F10.0,4I5)</u> - These cards are used to specify various forms of output data at selected times, and the last card must be for a time greater than TMAX, even though output will not be provided for that specific time.

TIME   =   Time at which output data will be provided.

ECHECK   =   A code which governs the printed output. The three following options are provided:

                  1)   If ECHECK is greater than 1000., the individual node data and element data will not be printed. Only system data such as cg positions, momenta, kinetic energies and average velocities are provided for the projectile, target and entire system.

                  2)   If ECHECK is positive (includes 0) and less than 1000., the system data and individual node data will be printed. Individual element data will be printed for all elements which have an equivalent strain [Equation (14)] equal to or greater than ECHECK. For example, if ECHECK = 0., all element data will be printed. If ECHECK = 0.5, only those elements with equivalent strains equal to or greater than 0.5 will have data printed. If ECHECK = 999., no element data will be printed.

                  3)   If ECHECK is negative, the system data and individual node data will be printed. The individual element data will be printed only for those elements which are plastic or failed. Data for the elastic elements will not be printed.

ISYS = 1 will write system data on Tape4. (Note: A program has not yet been written to read and plot these results.)

ILOAD = 1 will calculate internal loads in a cylindrical projectile. This option can only be used if NTOP, NBOT and NRING are properly defined in the Slide/Load Card.

ISAVE = 1 will write results on Tape2 for a possible restart run.

IPLOT = 1 will write results in Tape3 for a possible plot.

With the exception of the special shapes, this completes the description of the input data for an initial run. Four types of special shapes can be generated for either the projectile or the target. The node and element data for these special shapes are entered individually in the locations identified in Figure 10. The node data for each special shape require three cards, and the element data require one card for each special shape. A description of the special shapes data follows.

- <u>3 Node Cards for Each Rod Shape (4I5, 3F10. 0/5F10. 0/5F10. 0)</u> - The rod geometry descriptions are given in Figure 13. The rod is always generated in a vertical position about the z axis. Only half the rod is generated as shown, and restraints are provided normal to the plane of symmetry. The rotation of the rod for oblique impact is obtained with a Scale/Shift/Rotate Card.

1 = Identification number for rod geometry.

N1 = The node number of the centerline node on the top end of the rod. The nodes of the rod are numbered consecutively beginning with N1. It can be seen that the first ring on the top plane is defined by nodes N2-N6, in a counterclockwise direction. The second ring is defined by nodes N7-N15, the third ring by nodes

59

PLANES
OF NODES
1

NODE N1

RTOP1
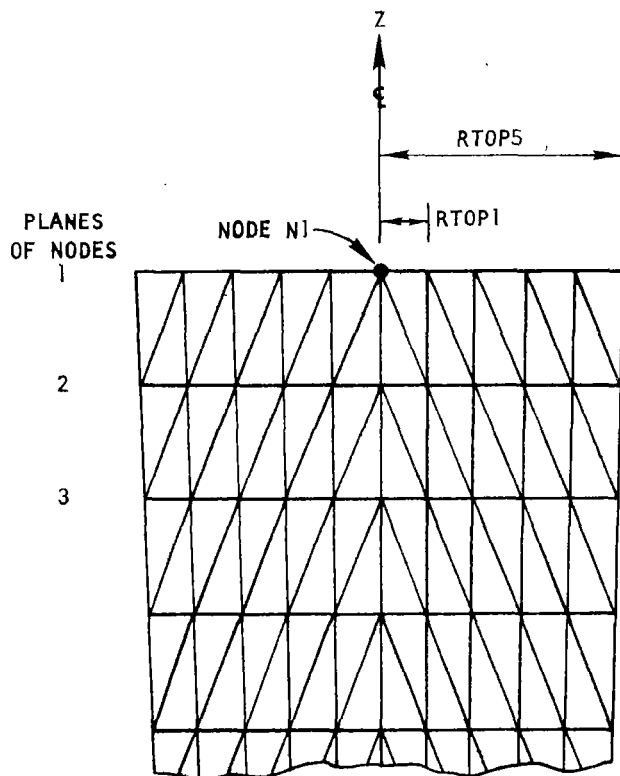
LAYERS
OF ELEMENTS

ZTOP

1

2

3

2

3

TOP VIEW

Y

Z = ZTOP

N50   N37   N24   N15   N6   N1   N2   N7   N16   N25   N38

RINGS → | 1 | 2 | 3 | 4 | 5 |

NLAY-1

NPLN-1

NPLN

NLAY

NODE [N1 + (NPLN -1) NPP]

RBOT1

RBOT5
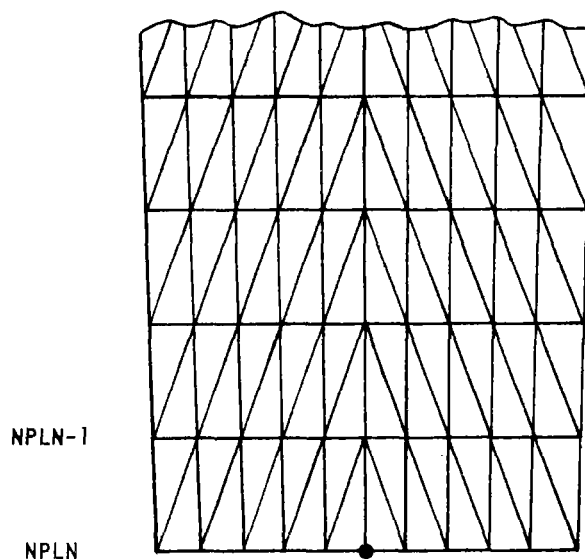
ZBOT

NUMBER OF RINGS (NRING)	NODES PER PLANE (NPP)	ELEMENTS PER LAYER (EPL)
1	6	12
2	15	48
3	24	96
4	37	156
5	50	228

Z

X

Y = 0

Figure 13. Geometry of Special Rod Shapes

60

N16-N24, the fourth ring by nodes N25-N37, and the
fifth ring by nodes N38-N50. The node numbers in the
plane of nodes below the top plane are numbered in the
same order as the top plane except each number is NPP
(Nodes Per Plane) greater than the node above it.
Values for NPP are dependent on the number of rings
and are shown in Figure 11. (Example: If N1 = 101
and there are four rings, the centerline node in the
second plane is N1 + NPP = 101 + 37 = 138.) With this
technique it is possible to identify readily the appro-
priate surface nodes for slave node designation and the
bottom centerline node, NBOT, for the internal loads
calculations.

NRING   =   The number of rings (1, 2, 3, 4 or 5) in the rod.

NPLN   =   The number of cross-sectional planes of nodes in the
              rod.

ZTOP   =   The z coordinate of the top of the rod.

ZBOT   =   The z coordinate at the bottom of the rod.

EXPAND   =   Factor by which the vertical distance between adjacent
              node changes. Factor applies from top to bottom.
              Same as described for the Projectile Node Data Cards.

RTOP1 - RTOP5   =   Radii of the rings at the top of the rod.

RBOT1 - RBOT5   =   Radii of the rings at the bottom of the rod.

Note: If it is not possible to describe the node geometry of the
         rod with a single shape, it is possible to use multiple
         shapes to form a single rod. The nodes must be numbered
         consecutively, and NRING must be the same for all the
         individual rod shapes.

61

● 3 Node Cards for Each Nose Shape (3I5, 5X, F10. 0/5F10. 0/5F10. 0) -
The nose geometry descriptions are given in Figure 14. The nose
shape is always generated in a vertical position (pointed downward)
about the z axis. Only half the nose shape is generated as shown, and
restraints are provided normal to the plane of symmetry. The node
geometry for the flat plane at the rod interface is not generated with the
nose generator and must therefore be generated with the rod generator.
The number of rings must be identical for the rod and the nose. The
surface nodes are also identified in Figure 14 so they can be designated
as slave nodes if necessary.

INOSE   =   2 identifies a rounded nose shape. If the length of the
              nose is equal to the radius, a spherical shape is gener-
              ated. When the length is not equal to the radius, the
              axial coordinates are scaled, and the various radii are
              not changed.

INOSE   =   3 identifies a conical nose shape.

N1   =   The node number of the centerline node at the top of the
              nose at the rod interface. This is identical to the bottom
              centerline node of the rod. This node is not the same as
              node N1 used for the rod shape. This node (and the other
              rod interface nodes) is not included in the nose generator
              and must be generated with the rod generator. It is used
              for reference such that the nodes can number in a consecu-
              tive manner.

NRING   =   Number of rings in the nose and the rod.

ZTOP   =   The z coordinate at the top of the nose. This is identical
              to ZBOT for the rod shape at the rod interface.

ROUNDED NOSE (INOSE = 2)   CONICAL NOSE (INOSE = 3)
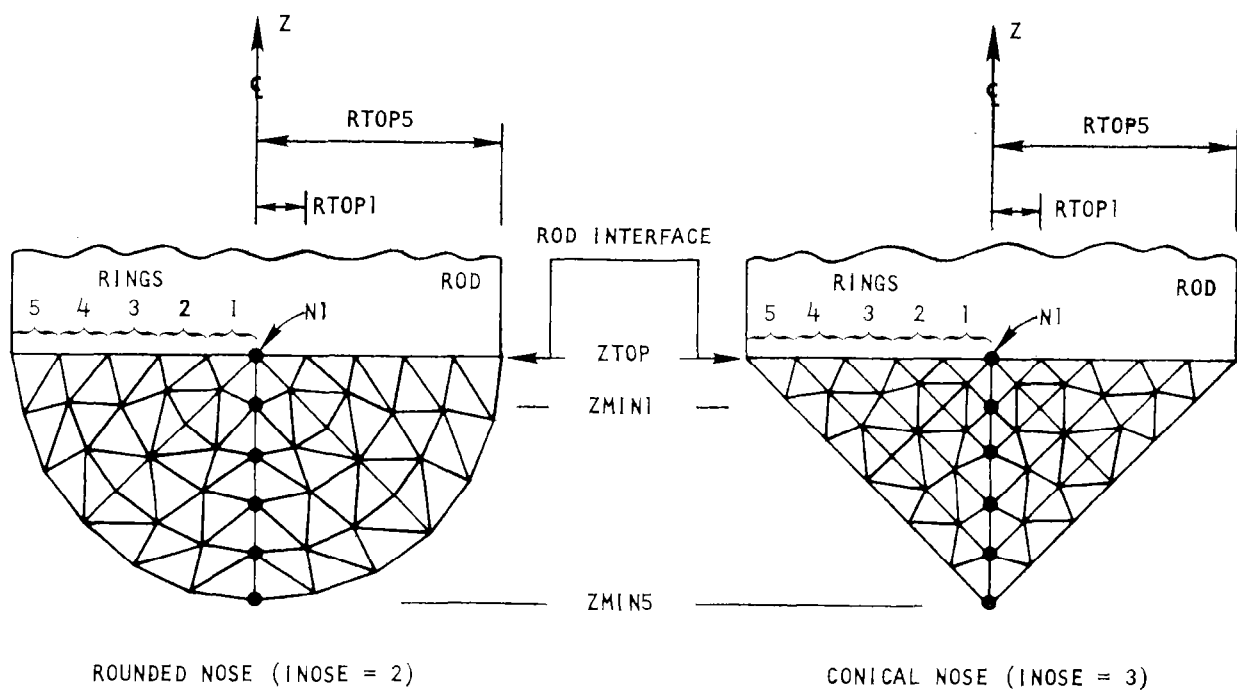
NUMBER OF RINGS (NRING)	NUMBER OF NODES[*]	NUMBER OF ELEMENTS	SURFACE NODES[*]
1	6	12	$(N1+6)$ - $(N1+11)$
2	30	96	$(N1+21)$ - $(N1+44)$
3	54	240	$(N1+54)$ - $(N1+77)$
4	108	468	$(N1+91)$ - $(N1+144)$
5	162	792	$(N1+158)$ - $(N1+211)$

[*] DOES NOT INCLUDE NODES AT ROD INTERFACE

Figure 14. Geometry of Special Nose Shapes

63

RTOP1 - RTOP5 = Radii of the rings at the top of the nose shape. These are generally equal to RBOT1 - RBOT5 for the rod shape at the rod interface.

ZMIN1 - ZMIN5 = Minimum coordinates for the rings in the nose shape (i.e., z coordinates of the nodes which lie on the z axis).

- **3 Node Cards for Each Flat-Plate Shape (2I5/6I5/6F10.0)** - The flat-plate descriptions are given in Figure 15. In all cases, the lines connecting the adjacent corner nodes are parallel to one of the three primary axes. The nodes are generated in rows parallel to the x axis and are numbered consecutively within each row, in the direction of the increasing x axis.

4 = Identification number for flat-plate geometry.

N1 = The node number of the corner with the minimum x and y coordinates and the maximum z coordinate.

NX = The number of nodes in the x direction. In Figure 15, NX = 9.

NY = The number of nodes in the y direction. In Figure 15, NY = 6.

NZ = The number of nodes in the z direction. In Figure 15, NZ = 5.

IDY = The node number increment between adjacent nodes when moving parallel to the y axis in the positive direction. If the entire plate is formed with one shape, then IDY should be equal to NX. If, however, the entire plate is to be formed with multiple plate shapes, then IDY should be equal to the total number of nodes along the x direction of the system of individual plate shapes. It is only necessary to use multiple shapes when the expansion factors must change along any of the three axes.

64

Figure 15. Geometry of Special Plate Shapes

65

IDZ = The node number increment between adjacent nodes when moving parallel to the z axis in the negative direction. If the entire plate is formed with one shape, then IDZ should be equal to NX · NY. For multiple shapes it should be equal to the total number of nodes in each x-y plane for the system of individual plate shapes.

IY = 1 gives restraint in the y direction if y = 0.

X-EXPAND = Factor by which the distance between adjacent nodes changes in the increasing x direction from X1 to XN. Same as described for the Projectile Node Data Cards.

Y-EXPAND = Factor by which the distance between adjacent nodes change in the increasing y direction from Y1 to YN.

Z-EXPAND = Factor by which the distance between adjacent nodes changes in the decreasing z direction from Z1 to ZN.

X1 = The x coordinate of node N1. This must be the minimum x coordinate of the plate shape.

Y1 = The y coordinate of node N1. This must be the minimum y coordinate of the plate shape.

Z1 = The z coordinate of node N1. This must be the maximum z coordinate of the plate shape.

XN = The x coordinate of NN. This must be the maximum x coordinate of the plate shape.

YN = The y coordinate of node NN. This must be the maximum y coordinate of the plate shape.

ZN = The z coordinate of node NN. This must be the minimum z coordinate of the plate shape.

66

- **Element Card for Each Rod Shape (10I5)** – This card generates elements for the rod shape illustrated in Figure 13 and described by the 3 Node Cards for Each Rod Shape.

1   =   Identification number for rod geometry.

N1   =   The node number of the centerline node on the top end of the rod.

NRING   =   The number of rings (1, 2, 3, 4 or 5) in the rod.

NLAY   =   The number of layers of elements in the rod.

ELE1   =   The element number of the first element in the rod. The elements are numbered consecutively and are generated in columns of composite brick elements beginning with top layer 1 and ending at bottom layer NLAY. The entire first ring of elements is generated before the second ring, etc., and the composite brick elements are generated in a counterclockwise manner for each ring of elements. The total number of elements in a rod shape is dependent on the number of layers (NLAY) and the number of elements per layer (EPL) shown in Figure 13. (Example: If NLAY = 10 and NRING = 3, the total number of elements is NLAY · EPL = 10 · 96 = 960.)

M1 - M5 =   Material numbers (1, 2, 3, 4 or 5) for the rings of the rod.

- **Element Card for Each Nose Shape (3I5, 5X, 6I5)** – This card generates elements for the nose shapes shown in Figure 14 and described by the 3 Node Cards for Each Nose Shape.

INOSE   =   2 identifies a rounded nose shape.

INOSE   =   3 identifies a conical nose shape.

N1 = The node number of the centerline node at the top of the nose at the rod interface.

NRING = Number of rings in the nose and the rod.

ELE1 = The element number of the first element in the nose shape. The elements are numbered consecutively from the inner ring to the outer ring.

M1 - M5 = Material numbers (1, 2, 3, 4 or 5) for the rings of the nose shape.

- Element Card for Each Flat-Plate Shape (3I5, 5X, 5I5) - This card generates elements for the flat-plate shape illustrated in Figure 15 and described by the 3 Node Cards for Each Flat Plate Shape.

4 = Identification number for flat-plate geometry.

N1 = The node number of the corner node shown in Figure 15.

4 = Identification number for flat-plate geometry.

ELE1 = The element number of the first element in the flat plate. The elements are numbered consecutively and are generated in columns of composite brick elements beginning at node N1. The columns of elements go in the direction of the increasing x axis. Each column of elements is to the positive y direction of the preceding column. After a layer is complete, the next lower layer is generated in a similar manner.

MATL = Material number (1, 2, 3, 4 or 5) of the flat plate.

NLX = Number of layers of composite brick elements in the x direction. The total number of nodes along the x direction must be NLX + 1. In Figure 15, NLX = 8.

NLY = Number of layers of composite brick elements in the y direction. The total number of nodes along the y direction must be NLY + 1. In Figure 15, NLY = 5.

NLZ   =   Number of layers of composite brick elements in the z direction. In Figure 15, NLZ = 4.

4.2 INPUT DATA FOR A RESTART RUN

A restart run is one which reads data from Tape2. These data must have been previously generated by setting ISAVE = 1 on a Data Output Card for an initial geometry run or a previous restart run. The descriptions which follow are for the input data in Figure 10.

- Identification Card (2I5, F10.0) –

  CASE   =   Case number for run identification. This does not have to be identical to that of the previous run.

  CYCLE =   The cycle number at which the restart occurs. The cycle numbers for which restart files are written, are given in the printed output of the previous run.

  CPMAX =   Central processor time (hours) at which the results will be written onto a restart tape and the run will stop. This feature will be bypassed if CPMAX = 0.

- Integration Time Increment Card (3F10.0) –

  DTMIN =   The minimum integration time increment which is allowed. If Δt from Equation (42) is less than DTMIN, the results will be written into the restart tape and the run will stop.

  STF   =   The fraction of the sound speed transit time used for the integration time increment. This is identical to C_t in Equation (42) and must be less than unity.

  TMAX   =   The maximum time the problem is allowed to run. This time refers to the dynamic response of the system, not the central processor time (CPMAX) defined in the Identification Card.

● <u>Data Output Cards (2F10.0, 4I5)</u> - Identical to the Data Output Cards for the Initial Run Input Data described in 4.1.

4.3 INPUT DATA FOR PLOTTING PROGRAM

A Calcomp plotting program has been written to plot the cross-sectional geometry of the x-z plane at y=0. Plots can be obtained for various times by setting IPLOT = 1 on the Data Output Cards. This will write the required plotting data on Tape3 so they can be read by the plotting program. The vertical z axis is currently 10 inches long, and the horizontal x axis is as specified. Each plot requires one card, and the cards must be arranged in order of increasing cycle number. The last card, which will stop the program, should have four nines (9999) in columns 2-5.

● <u>Plot Card (2I5, 4F10.0, 3A6, IX, I1, 4X, I4, 4X, I4)</u> -

CASE   =   The same case number as used on the Identification Card for the run being plotted. The last card in the data deck should have CASE = 9999. (Columns 1-5)

CYCLE   =   The cycle number of the plot which is desired. The cycle numbers of the data written on Tape3 are given in the printed output of the main program. (Column 6-10)

ZMAX   =   The maximum z coordinate to be included in the plot. Any elements having a z coordinate greater than ZMAX will not be plotted. (Columns 11-20)

ZMIN   =   The minimum z coordinate to be included in the plot. Any elements having a z coordinate less than ZMIN will not be plotted. The vertical z axis is 10 inches long and extends from ZMAX down to ZMIN. (Columns 21-30)

XMAX   =   The maximum x coordinate to be included in the plot. Any elements having an x coordinate greater than XMAX will not be plotted. (Columns 31-40)

70

XMIN   =   The minimum x coordinate to be included in the plot.
Any elements having an x coordinate less than XMIN will
not be plotted.   The length of the horizontal x axis can
vary.   This axis will have the same scale factor as the
vertical z axis.   (Columns 41-50)

TITLE =   The title which is written on the plot.   The time and cycle
number are also written on the plot.   (Columns 51-68)

IE   =   1 will write "E" at the center of all elements which are
in the elastic range.   Will not write if it is left blank.
(Column 70)

IP   =   1 will write a "P" at the center of all elements which are
in the plastic range.   Will not write if it is left blank.
(Column 75)

IF   =   1 will write an "F" at the center of all elements which
are failed in shear and tension.   Will not write if it is
left blank.   (Column 80)

4.4 SAMPLE INPUT DATA

A listing of input data for a sample run is shown in Figure 16.   The projec-
tile is a long rod, with a hemispherical nose, impacting a flat-plate target
at an oblique angle.   Consistent units (pound-inch-second) are used for the
input data.   The projectile (MATL1) and the target (MATL3) are similar
steels, with the projectile having slightly higher yield and ultimate stresses.
The projectile geometry is generated with one special rod shape and one
special nose shape.   The total length is 4.0 inches and the diameter is 0.4
inch.   The target requires six special flat-plate shapes for the nodes since
the expansion factors (X-EXPAND, Y-EXPAND, Z-EXPAND) are not con-
stant for the x and y directions.   Only one special element card is required
for the plate, however.   The length of the plate is 8.0 inches, the

71

```
500      0        .5
        .0073                        .0073
      400000.                      400000.
    30000000,                    30000000,
        .3                           .3
        0.                           0.
     200000,                      150000.
     240000.                      180000.
        .1                           .1
      60000,                       60000,
        0,                           0.
        0,                           0.
        0.                           0.
        1,                           1.
        0,                           0.
    23000000,                    23000000,
    43000000,                    45000000.
     7000000,                     7000000.
        1,2                          1,2
        .5                           .5
        4,                           4,
      999.                         999.
      999,                         999,
      999,                         999,
       50,                          50,

        1.          1.          1,          0,        .21       -60.

    1    1    3    20         4,        .2        .01
        .067       .133        .2
        .067       .133        .2
    2   457    3              .2
        .067       .133        .2
        .133       .067        0,

        1.          1.          1,          0,         0,         0,

    4   541
    6     4    6    27   243    1        .67        1.         1,
        -4,         0,          0,       -1,        .25       -.4
    4   542
   15     4    6    27   243    1        1,         1.         1,
        -.85        0,          0,        .85        .25       -.4
    4   562
    6     4    6    27   243    1        1,5        1.         1,
        1,          0,          0,        4,         .25       -.4
    4   649
    6     5    6    27   243    0        .67        1,5        1,
        -4,         .4          0,       -1,         3,        -.4
    4   655
   15     5    6    27   243    0        1.         1,5        1.
        -.85        .4          0,        .85        5,        -.4
    4   670
    6     5    6    27   243    0        1,5        1,5        1.
        1.          .4          0,        4,         3,        -.4

    1    1    3    19    1    1    1    1
    2  457    3        2001    1    1    1

    4  541    4        3001    3    26    6    5

    1    0    1   457    3
    1   21    5   108
  544  545  546  547  548  549  550  551  552  553  554  555  556  557  558  559
  560  561  562  563  564
  571  572  573  574  575  576  577  578  579  580  581  582  583  584  585  586
  587  588  589  590  591
  598  599  600  601  602  603  604  605  606  607  608  609  610  611  612  613
  614  615  616  617  618
  625  626  627  628  629  630  631  632  633  634  635  636  637  638  639  640
  641  642  643  644  645
  652  653  654  655  656  657  658  659  660  661  662  663  664  665  666  667
  668  669  670  671  672
  116  140  164  188  212  236  260  284  308  332  356  380  404  428  452  476
  117  141  165  189  213  237  261  285  309  333  357  381  405  429  453  477
  118  142  166  190  214  238  262  286  310  334  358  382  406  430  454  478
  119  143  167  191  215  239  263  287  311  335  359  383  407  431  455  479
  120  144  168  192  216  240  264  288  312  336  360  384  408  432  456  480
  472  473  474  475  511  512  513  514  515  516  517  518  519  520  521  522
  523  524  525  526  527  528  529  530  531  532  533  534
    51500.        0,      -30000,         0,         0,         0,
   .00000005   .000001  .00000001        .5    .00000001
        0,         -1,          0    0    1    1
        1.
```

Figure 16. Input Data for the Sample Problem

72

half-width is 3.0 inches and the thickness is 0.4 inch. This problem contains 1992 nodes and 8304 elements. The master sliding surface is defined by five rows of 21 nodes for a total of 105 master nodes. A total of 108 surface nodes on the nose and lower portion of the rod are designated as slave nodes. The impact conditions are 60 degrees from normal at a net velocity of 60,000 inches/second. A Calcomp plot is shown in Figure 17 for the cross-sectional geometry at cycle 1.

4.5 OUTPUT DATA DESCRIPTION

The output data are generally clearly described using the terminology of this report. A summary of the printed output for an initial run is as follows:

- Material data are printed for the input and generated data.

- All the geometric input data are printed in a form similar to that used to read the data.

- For each element, the four nodes, the volume and material number are printed.

- For each node, the initial coordinates, mass and restraints are printed. The slave nodes are identified by adding a "1" before the XYZ restraint. (Example: If the XYZ restraint is 110, the node is restrained in the x and y directions. If the XYZ restraint is 1110, it is a slave node with the same restraints.)

- A summary of the initial geometry and impact conditions is printed. Included are the number of nodes and elements, mass, cg positions, velocities, momenta, kinetic energies and integration time increment data.

SAMPLE PROBLEM
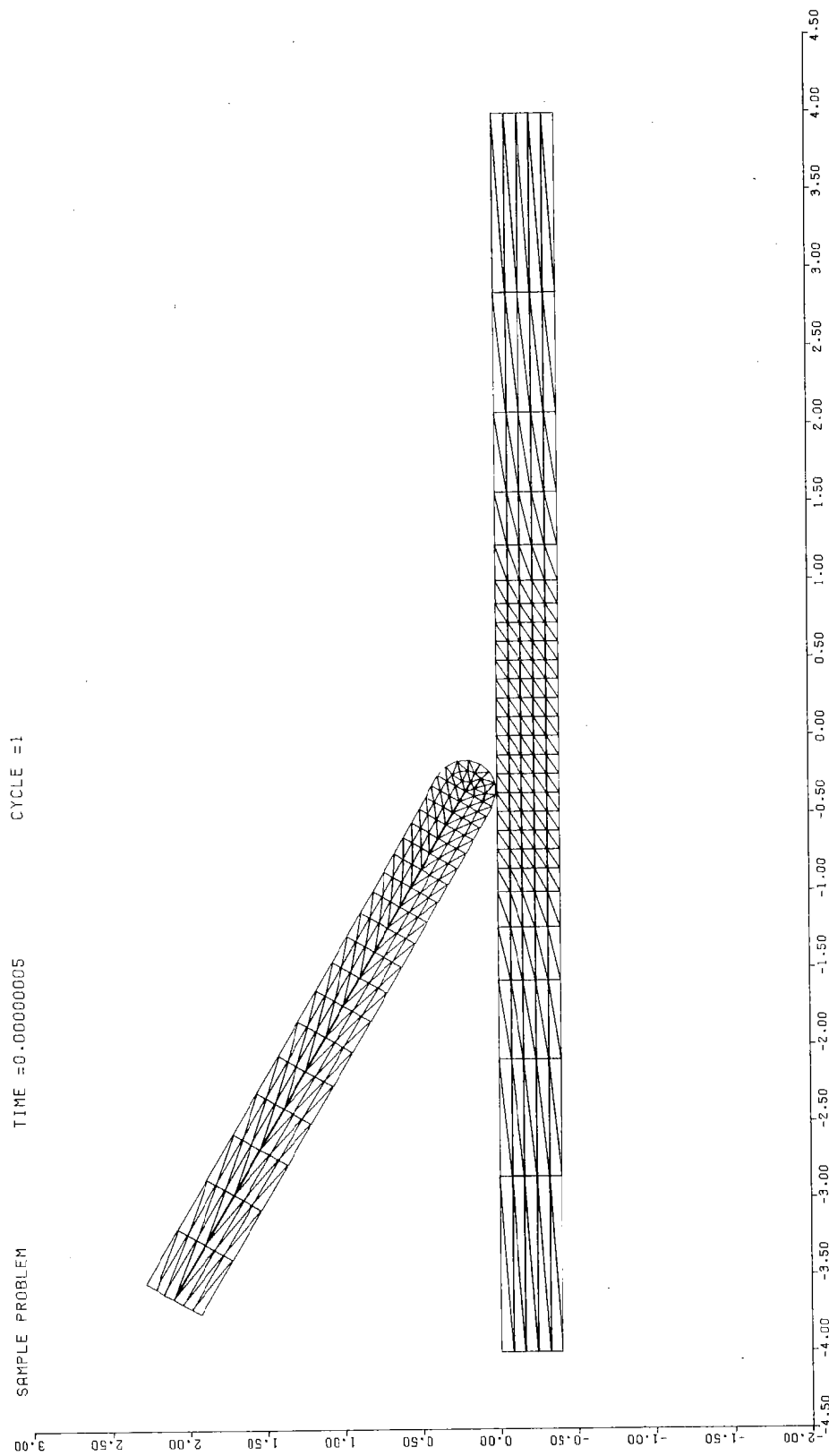
TIME =0.00000005

CYCLE =1

Figure 17. Plot of the Sample Problem

- For each integration time increment selected data are printed. These consist of cycle number (CYCLE), the time (TIME), the integration time increment (DT), the element number which governs the time increment (ECRIT), the total system kinetic energy (TOTAL K. E.), the projectile momenta (PROJ MVX, PROJ MVY, PROJ MVZ), the plastic work in the projectile (PROJ PLAST), the plastic work in the total system (TOT PLAST), and the total energy in the system (TOT ENERGY). If ECRIT = 0, the integration time increment calculated by Equation (42) is either greater than DTMAX, or greater than 1.1 times the integration time increment for the previous cycle. If the total energy in the system remains constant, the approximate formulation for the internal energy in Equation (56) is adequate.

- A summary of data for the projectile, target and total system (projectile and target) is printed for selected times specified on the Data Output Cards. These data consist of mass, cg positions, linear momenta, linear velocities, angular momenta and angular velocities.

- Node data are printed at the selected times specified on the Data Output Cards if ECHECK is less than 1000. These data include the node number (NODE), the coordinates (X, Y, Z), the velocities (XDOT, YDOT, ZDOT) and the accelerations (XDD, YDD, ZDD). If the acceleration data are not printed, this indicates that the node is a slave node which is currently in contact with the master surface.

- Element data may be printed at the selected times specified on the Data Output Cards if ECHECK is less than 1000. If ECHECK is negative, only the plastic and failed element data are printed. For positive ECHECK less than 1000, only those elements with an equivalent strain equal to or greater than ECHECK, will have

their data printed. If the element is plastic range, these data consist of the element number (ELE), the normal strains (EX, EY, EZ) and shear strains (EXY, EXZ, EYZ) given by Equations (7) to (12), the equivalent strain (EBAR) given by Equation (14), the equivalent strain rate (EDOT), the volumetric strain (DVOL) given by Equation (13), the equivalent tensile strength (SEFF) given by Equation (31), the hydrostatic pressure (PRESURE) given by Equation (32), the artifical viscosity [Q(VIS)] given by Equation (33), the normal deviator stresses (SX, SY, SZ) given by Equations (25) to (27), and the shear stresses (SXY, SXZ, SYZ) given by Equations (28) to (30). If the element is in the elastic range, EDOT is set equal to 1, and SEFF is the equivalent stress given by Equation (21). Also, the normal elastic stresses of Equations (15) to (17) are presented in the form of a hydrostatic pressure and deviator stresses.

● Internal loads can be obtained for slender projectiles at selected times if the nodal geometry is consistent with the geometry generator for rods and if ILOAD = 1 on the Data Output Cards. The output is given along the centerline of the projectile from nodes NTOP to NBOT as specified on the Slide/Load Card. Included are the node numbers (NODE), the coordinates of the nodes (X, Z), the bending moment (BENDING MOMENT), the x and z forces (X LOAD, Z LOAD) the transverse shear force (SHEAR LOAD) and the axial force (AXIAL LOAD). The bending moment is calculated at the node positions and acts on the lower (forward) end of the upper (aft) portion of the projectile as shown in Figure 18. A clockwise moment is positive when looking along the y axis. The x and y forces are calculated for the increments between the nodes and are positive when applied in the positive x and z directions. The shear force is positive when it acts in a
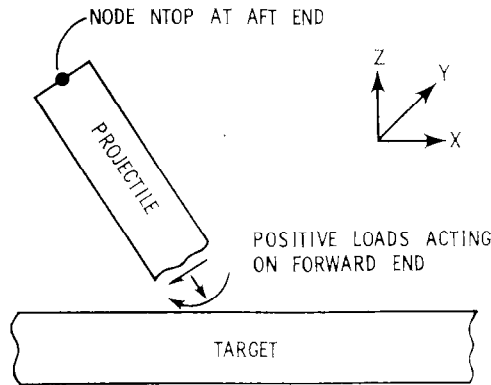
Figure 18. Sign Convention for Internal Projectile Loads

clockwise direction about the upper (aft) end of the projectile
when looking along the y axis. The axial force is positive when
the projectile is in tension. The results are valid only along
the free portion of the projectile, and are not valid for the por-
tions which are in contact with the target.

4.6 DIAGNOSTICS

The following diagonistics are provided.

- CP TIME LIMIT EXCEEDED - This means the central processor
  time is greater than specified by CPMAX, on the Identification
  Card. The results are written on the restart tape and the run
  is discontinued.

- MINIMUM TIME INCREMENT HAS BEEN VIOLATED - This
  means the time increment calculated by Equation (42) is less
  than specified by DTMIN on the Integration Time Increment
  Card. The results are written on the restart tape and the
  run is discontinued. If it is desired to continue the run to
  later times, DTMIN must be decreased for the next restart
  run.

77

- ENERGY CHECK INDICATES NUMERICAL INSTABILITY - This means the kinetic energy of the system is at least 10 percent greater than the initial kinetic energy. Since this is not physically possible, the run must be numerically unstable.

- END OF RESTART TAPE - This means a restart run has been attempted, but the restart tape does not have data for the cycle number specified on the Identification Card.

4.7 CENTRAL PROCESSOR TIME ESTIMATES

For a limited number of problems run on a Honeywell 6080 Computer, the program has used approximately 0.025 central processor second per node per cycle.

4.8 CENTRAL MEMORY STORAGE REQUIREMENTS AND ALTERATIONS

The program is currently limited to five materials, 2000 nodes and two sliding surfaces, each with a maximum of 300 slave nodes and 300 master nodes. The element blocks contain data for 200 elements. This requires 69K Central Memory Storage on a Honeywell 6080 Computer. To increase the capability of the program for problems involving more than 2000 nodes, it is necessary to increase the size of the node arrays in Subroutines ELEG, GEOM, GPLOT, LOAD, LOOP, NODEG, RECALL, SAVE, SDATA, SLIDE and START. The sliding surface arrays are contained in Subroutines GEOM, LOOP, RECALL, SAVE and SLIDE. If it is desired to change the block size for the elements, the element arrays are contained in Subroutines ELEG, GEOM, GPLOT, LOOP, RECALL, SAVE and SLIDE. If the size of the element arrays is changed, it is necessary to redefine NBSIZE (Card 37 in Subroutine GEOM) to be equal to the dimension of the element arrays.

REFERENCES

1. Boresi, A. P., Elasticity in Engineering Mechanics, Prentice-Hall, Englewood Cliffs, N. J., 1965.

2. Crandall, S. H., and Dahl, N. C., An Introduction to the Mechanics of Solids, McGraw-Hill, New York, 1959.

3. Schlichting, H., Boundary Layer Theory, McGraw-Hill, New York, 1955.

4. Kohn, B. J., "Compilation of Hugoniot Equations of State," Air Force Weapons Laboratory Report AFWL-TR-69-38, Kirtland AFB, N. M., April 1969.

5. Von Neumann, J. and Richtmyer, R. D., "A Method for the Numerical Calculation of Hydrodynamic Shocks," Journal of Applied Physics, Vol. 21, 1950.

6. Wilkins, M. L., "Calculation of Elastic-Plastic Flow," Methods in Computational Physics, Vol. 3, edited by B. Alder, S. Fernback and M. Rotenberg, Academic Press, New York, N. Y., 1964.

7. Walsh, R. T., "Finite Difference Methods," Dynamic Response of Materials to Intense Impulsive Loading, edited by P. C. Chou and A. K. Hopkins, Air Force Materials Laboratory, 1972.

8. Johnson, G. R., "Analysis of Elastic-Plastic Impact Involving Severe Distortions," Journal of Applied Mechanics, ASME, Vol. 98, No. 3, September 1976.

9. Backman, M. E. and Finnegan, S. A., "Dynamics of the Oblique Impact and Ricochet of Nondeforming Spheres Against Thin Plates," Naval Weapons Center Report NWC-TP-5844, September, 1976.

10. Johnson, G. R., "High Velocity Impact Calculations in Three Dimensions," Journal of Applied Mechanics, ASME, Vol. 99, No. 1, March 1977.

11. Johnson, G. R., "A New Computational Technique for Intense Impulsive Loads," Proceedings of Third International Symposium on Ballistics, Karlsruhe, Germany, March 1977.

DISTRIBUTION LIST

No. of Copies	Organization
12	Commander Defense Documentation Center ATTN: DDC-TCA Cameron Station Alexandria, VA 22314
1	Director Defense Nuclear Agency ATTN: MAJ Spangler Arlington, VA 22209
1	Director Defense Advanced Research Projects Agency ATTN: Tech Info 1400 Wilson Boulevard Arlington, VA 22209
1	Commander US Army Materiel Development and Readiness Command ATTN: DRCDMA-ST 5001 Eisenhower Avenue Alexandria, VA 22333
1	Commander US Army Aviation Systems Command ATTN: DRSAV-E 12th and Spruce Streets St. Louis, MO 63166
1	Director US Army Air Mobility Research and Development Laboratory Ames Research Center Moffett Field, CA 94035
2	Commander US Army Electronics Command ATTN: DRSEL-HL-CT, S.Crossman DRSEL-RD Fort Monmouth, NJ 07703

No. of Copies	Organization
2	Commander US Army Missile Research and Development Command ATTN: DRDMI-R DRDMI-RBL Redstone Arsenal, AL 35809
1	Commander US Army Tank Automotive Development Command ATTN: DRDTA-RWL Warren, MI 48090
3	Commander US Army Mobility Equipment Research & Development Command ATTN: Tech Docu Cen, Bldg. 315 DRDME-RZT Dr. J. Bond Fort Belvoir, VA 22060
1	Commander US Army Armament Materiel Readiness Command Rock Island, IL 61201
4	Commander US Army Armament Research and Development Command ATTN: Mr. V. Guadagno Mr. R. Davitt B. Knutelsky G. Demitrak Dover, NJ 07801
1	Commander US Army Watervliet Arsenal ATTN: SARWV-RDD-SE, P. Vottis Watervliet, NY 12189
1	Commander US Army Harry Diamond Labs ATTN: DRXDO-TI 2800 Powder Mill Road Adelphi, MD 20783

DISTRIBUTION LIST

No. of Copies	Organization

No. of Copies	Organization

5 Commander
US Army Materials and
Mechanics Research Center
ATTN: DRXMR-T, Mr. J. Bluhm
DRXMR-T, D. Roylance
DRXMR-T, Dr. A.F. Wilde
Dr. J. Mescall
DRXMR-ATL
Watertown, MA 02172

1 Commander
US Army Natick Research
and Development Center
ATTN: DRXRE, Dr. E. Sieling
Natick, MA 01762

1 Director
US Army TRADOC Systems
Analysis Activity
ATTN: ATAA-SA
White Sands Missile Range
NM 88002

1 Deputy Assistant Secretary
of the Army (R&D)
Department of the Army
Washington, DC 20310

1 HQDA (DAMA-ARP)
Washington, DC 20310

1 HQDA (DAMA-MS)
Washington, DC 20310

1 Commander
US Army Research Office
ATTN: Dr. E. Saibel
P. O. Box 12211
Research Triangle Park
NC 27709

1 Chief of Naval Research
ATTN: Code ONR 439
N. Perrone
Washington, DC 20360

3 Commander
US Naval Air Systems Command
ATTN: AIR-604
Washington, DC 20360

3 Commander
US Naval Ordnance Systems
ATTN: ORD-9132
Washington, DC 20360

2 Commander
US Naval Air Development
Center, Johnsville
Warminster, PA 18974

1 Commander
US Naval Missile Center
Point Mugu, CA 93041

1 Commander and Director
David W. Taylor Naval Ship
Research & Development Center
Bethesda, MD 20084

2 Commander
US Naval Surface Weapons Center
Silver Spring, MD 20910

1 Commander
US Naval Surface Weapons Center
ATTN: Code TX, Dr. W.G. Soper
Dahlgren, VA 22448

3 Commander
US Naval Weapons Center
ATTN: Code 4057
Code 5114, E. Lundstrom
Code 6031, Mr.M.Backman
China Lake, CA 93555

No. of Copies	Organization	No. of Copies	Organization
4	Commander US Naval Research Laboratory ATTN: Mr. W. J. Ferguson Mr. J. Baker Dr. H. Pusey Dr. F. Rosenthal Washington, DC 20375	4	Director National Aeronautics and Space Administration Langley Research Center Langley Station Hampton, VA 23365
1	Superintendent US Naval Postgraduate School ATTN: Dir of Lib Monterey, CA 95940	1	Director National Aeronautics and Space Administration Manned Spacecraft Center ATTN: Lib Houston, TX 77058
2	ADTC/DLJW (MAJ D. Matuska, LTC J. Osborn) Eglin AFB, FL 32542	2	Aerospace Corporation ATTN: Mr. D. Babin Dr. E. B. King P. O. Box 95085 Houston, TX 77058
1	AFFDL (FDT) Wright-Patterson AFB, OH 45433		
1	AFML (Dr. T. Nicholas) Wright-Patterson AFB, OH 45433	1	Boeing Aerospace Company ATTN: Mr. F. G. Blaisdell (M.S. 40-25) Seattle, WA 98124
3	ASD (YH/EX, John Rievley; XRHD, Gerald Bennett; ENFTV, Matt Kolleck) Wright-Patterson AFB, OH 45433	2	Dupont Experimental Labs ATTN: Mr. J. Lupton Dr. C. Zweben Wilmington, DE 19801
1	Director Lawrence Livermore Laboratory ATTN: Dr. R.H. Toland, L-424 P. O. Box 808 Livermore, CA 94550	1	Falcon R&D ATTN: Mr. E. Miller 1225 S. Huron Street Denver, CO 80223
1	Director Jet Propulsion Laboratory ATTN: Lib (TD) 4800 Oak Grove Drive Pasadena, CA 91103	2	Falcon R&D, Ober Facility ATTN: Mr. D. Malick Mr. J. Wilson 696 Fairmount Avenue Baltimore, MD 21204
1	Headquarters National Aeronautics and Space Administration Washington, DC 20546	1	President General Research Corporation ATTN: Lib McLean, VA 22101

DISTRIBUTION LIST

No. of Copies	Organization

3	Honeywell, Inc.
	Government and Aerospace
	  Products Division
	ATTN: Mr. J. Blackburn
	       Dr. G. Johnson
	       Mr. R. Simpson
	600 Second Street, NE
	Hopkins, MN 55343

1	Lockheed Huntsville ATTN: Dr. E. A. Pickelsimer P. O. Box 1103 Huntsville, AL 35809
1	Lockheed Corporation Department 8114 ATTN: Dr. C. E. Vivian Sunnyvale, CA 94087

1	McDonnell-Douglas Astronautics
	  Company
	ATTN: Mail Station 21-2
	       Dr. J. Wall
	5301 Bolsa Avenue
	Huntington Beach, CA 92647

3	Physics International Company
	ATTN: Dr. D. Orphal
	       Dr. E. T. Moore
	       Dr. M. Chawla
	2700 Merced Street
	San Leandro, CA 94577

3	Sandia Laboratories
	ATTN: Dr. W. Herrmann
	       Dr. L. Bertholf
	       Dr. J. W. Nunziato
	Albuquerque, NM 87115

2	Systems, Science & Software ATTN: Dr. R. Sedgwick Ms. L. Hageman P. O. Box 1620 La Jolla, CA 92038

No. of Copies	Organization

2	California Institute of Tech
	Division of Engineering and
	  Applied Science
	ATTN: Dr. J. Miklowitz
	       Dr. E. Sternberg
	Pasadena, CA 91102

2	The Johns Hopkins University ATTN: Dr. J. Bell Dr. R. Green 34th and Charles Streets Baltimore, MD 21218
1	Drexel University Department of Mechanical Engineering ATTN: Dr. P. C. Chou 32nd and Chestnut Streets Philadelphia, PA 19104
1	Lehigh University Center for the Application of Mathematics ATTN: Dr. R. Rivlin Bethlehem, PA 18015

2	Massachusetts Institute of
	  Technology
	ATTN: Dr. R. Probstein
	       Dr. J. Dugundji
	77 Massachusetts Avenue
	Cambridge, MA 02139

1	North Carolina State Univ Dept of Engineering Mechanics ATTN: Dr. W. Bingham P. O. Box 5071 Raleigh, NC 27607
1	Forrestal Research Center Aeronautical Engineering Lab Princeton University ATTN: Dr. A. Eringen Princeton, NJ 08540

DISTRIBUTION LIST

No. of Copies	Organization	No. of Copies	Organization
2	Rice University P. O. Box 1892 ATTN: Dr. Bowen Dr. A. Miele Houston, TX 77001	4	University of California Los Alamos Scientific Lab ATTN: Dr. R. Karpp Dr. J. Dienes Dr. L. Germain Dr. B. Germain P. O. Box 808 Livermore, CA 94550
3	Southwest Research Institute Dept of Mechanical Sciences ATTN: Dr. U. Lindholm Dr. W. Baker Dr. P. H. Francis 8500 Culebra Road San Antonio, TX 78228	1	University of Dayton Univ of Dayton Rsch Institute ATTN: Mr. H. F. Swift Dayton, OH 45406
1	Stanford Research Institute Poulter Laboratory 333 Ravenswood Avenue Menlo Park, CA 94025	3	University of Delaware Dept of Mechanical Engineering ATTN: Prof. J. Vinson Prof. J. Nowinski Dr. B. Pipes Newark, DE 19711
3	University of Arizona Civil Engineering Department ATTN: Dr. D. A. DaDeppo Dr. R. Richard Dr. R. C. Neff Tucson, AZ 85721	2	University of Denver Denver Research Institute ATTN: Mr. R. F. Recht Mr. T. W. Ipson 2390 South University Blvd Denver, CO 80210
2	University of California ATTN: Dr. M. Carroll Dr. P. Naghdi Berkeley, CA 94704	1	University of Illinois Department of Theoretical and Applied Mechanics Urbana, IL 61801
1	University of California Dept of Aerospace and Mechanical Eng Sciences ATTN: Dr. Y. C. Fung P. O. Box 109 La Jolla, CA 92037	1	University of Iowa ATTN: Dr. K. Valanis Iowa City, IA 50010
2	University of California Department of Mechanics ATTN: Dr. R. Stern Dr. S. B. Dong 504 Hilgard Avenue Los Angeles, CA 90024	2	University of Maryland Department of Mechanical Eng ATTN: Prof. Y. Yang Dr. J. Dally College Park, MD 20742

DISTRIBUTION LIST

No. of Copies	Organization	No. of Copies	Organization
1	University of Minnesota Dept of Engineering Mechanics ATTN: Dr. R. Fosdick Minneapolis, MN 55455	2	Yale University ATTN: Dr. B. Chu Dr. E. Onat 400 Temple Street New Haven, CT 96520
2	University of Texas Dept of Engineering Mechanics ATTN: Dr. C. H. Yew Dr. J. T. Oden Austin, TX 78712		
			Aberdeen Proving Ground
1	University of Washington Dept of Mechanical Engineering ATTN: Prof. J. Chalupnik Seattle, WA 98105		Marine Corps Ln Ofc Dir, USAMSAA Cdr, USATECOM ATTN: Mr. W. Pless Mr. S. Keithley
1	Washington State University Department of Physics ATTN: Dr. G. E. Duvall Pullman, WA 99163		